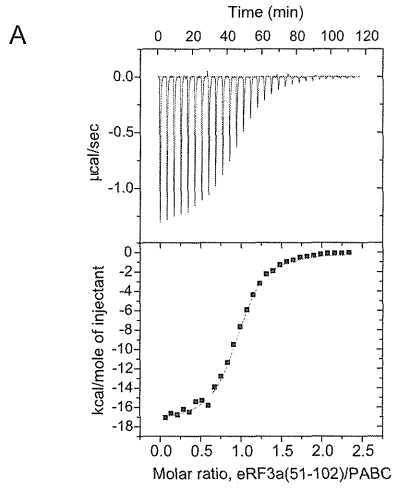

B

PAM2-1 PAM2-2

eRF3a(79-94)	GPLGSNVHAAEFVPSFLRGPA
eRF3a(76-94)	FVPNVHAAEFVPSFLRGPA
eRF3a(73-94)	AKPFVPNVHAAEFVPSFLRGPA
eRF3a(64-82)	GPLGSAFSRQLNVNAKPFVPNVHA
eRF3a(64-78)	AFSRQLNVNAKPFVP
eRF3a(64-75)	AFSRQLNVNAKP
eRF3a(64-81,76-94)	AFSRQLNVNAKPFVPNVHFVPNVHAAEFVPSFLRGPA

FIGURE 3. Isothermal titration microcalorimetric analyses of the interactions between eRF3a fragments and PABC. (*A*, *upper* panel) Trace of the calorimetric titration of 29 10-µL aliquots of eRF3a(51–102) into the cell containing PABC. (*Lower* panel) The integrated binding isotherm obtained from the experiment was fitted using a single-site model. The parameters obtained from the best fit (solid line) with the error values calculated from the fittings are summarized in Table 1. (*B*) Amino acid sequence alignment of the peptides used for the ITC analyses. PAM2-N (blue), PAM2-C (cyan), and their overlapping region (red). (Gray) Sequences derived from cloning artifacts.

L585, M596, and V607 in Fig. 5A) upon binding to eRF3a(51–102) ranged from 30 to 120 Hz, indicating that the chemical exchange rate between states is on the order of 10^2/sec at the experimental temperature of 303 K.

Three-dimensional structures of PABC in complex with PAM2-N and PAM2-C

To describe the two exchanging states, we determined the three-dimensional structures of each complex: PABC in complex with eRF3a(64–82; PAM2-N) and eRF3a(73–94; PAM2-C). Statistics for these structures are summarized in Table 2. Figure 6 shows the solution structures of PABC–eRF3a(64–82) and PABC–eRF3a(73–94). The structure of the N-terminal helix 1 was less well defined due to the fewer NOEs observed for this region, suggesting that helix 1 is loosely packed with other helices. The region containing helices 2–5 contains hydrophobic pockets, one between helices 2 and 3 (N-pocket), consisting of L585, I588, V607, and A610, and another between helices 3 and 5 (C-pocket), consisting of G563, F567, T582, and L586 (Fig. 6C,D; Kozlov et al. 2004). These pockets play critical roles in recognition of the PAM2 hydrophobic residues.

A specific tertiary structure is induced in each PAM2 motif by binding to PABC. In spite of differences in the sequences at positions 1–3, 6, 8, and 9 of PAM2-N and PAM2-C (Fig. 1), both motifs adopt similar backbone structures in which the residues at positions 4–7 (N70, V71, N72, and A73 for PAM2-N and N79, V80, H81, and A82 for PAM2-C) form a type-II β-turn. The side chains of V71 and V80 at position 5 face outside from the turn, interacting with V613 and L614 within helix 5 of PABC. No notable intermolecular interaction was observed for residues N72 and H81 at position 6, whose side chains are exposed to the solvent, suggesting that a hydrophilic residue is preferable for this position. While the PABC-bound PAM2 of Paip1 and 2 contains two β-turn structures, only one β-turn was observed for the PAM2 motifs of eRF3.

The residues at position 10 of PAM2-N and C, F76 and F85, are accommodated in the N-pocket of PABC. The hydrophobic residues at position 3, L69 in PAM2-N and P78 in PAM2-C, bind to the C-pocket. In addition to these

TABLE 1. Thermodynamic parameters for interaction of the eRF3a fragments with PABC

eRF3a residues	Binding stoichiometry (eRF3/PABC)	K_d (µM)	ΔH (kcal/mol)	ΔS (cal mol^{-1} K^{-1})
1–207	0.851 ± 0.003	2.3 ± 0.1	−22.84 ± 0.09	−50.84
51–102	1.052 ± 0.003	0.69 ± 0.04	−16.7 ± 0.1	−27.7
64–94	0.909 ± 0.003	0.42 ± 0.02	−17.3 ± 0.1	−28.9
64–94(F76A)	0.94 ± 0.03	11.1 ± 0.09	−13.0 ± 0.6	−20.8
64–94(F85A)	0.888 ± 0.009	0.82 ± 0.08	−17.2 ± 0.2	−30.0
64–94(F76A/F85A)[a]	N.D.	N.D.	N.D.	N.D.
64–82	1.004 ± 0.001	0.82 ± 0.02	−22.63 ± 0.03	−48.07
64–78	1.082 ± 0.003	5.4 ± 0.1	−16.67 ± 0.06	−31.83
64–75[a]	N.D.	N.D.	N.D.	N.D.
73–94	1.184 ± 0.008	2.9 ± 0.2	−22.2 ± 0.2	−49.14
76–94	1.047 ± 0.004	5.5 ± 0.2	−21.2 ± 0.1	−47.1
79–94	1.16 ± 0.01	16.7 ± 0.6	−31.94 ± 0.02	−85.28
64–81, 76–94	0.502 ± 0.002	3.1 ± 0.9	−44.4 ± 0.2	−124

The errors were obtained by the least-square fitting.
[a]Sufficient heat exchange was not detected.

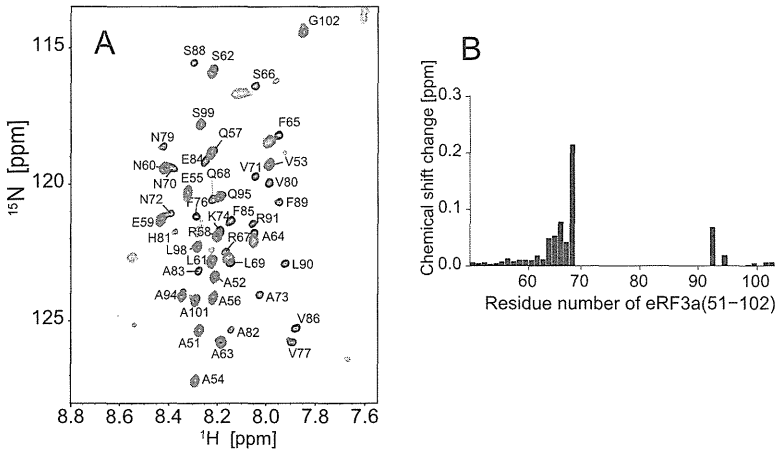

FIGURE 4. Chemical shift changes of uniformly ^{15}N-labeled eRF3a(51–102) upon addition of PABC. (*A*) Overlay of the ^{1}H–^{15}N HSQC spectra of ^{15}N-labeled eRF3a(51–102) in the absence (black) and presence (red) of PABC. (*B*) The chemical shift changes are plotted versus the residue number of eRF3a. Signals from residues 70–92 disappeared upon addition of PABC.

interactions, which were observed for the PAM2 motifs in Paip1 and 2 (Kozlov et al. 2004), the C-pocket also accommodates a phenylalanine side chain at the N-terminal position −2 of PAM2-N (F65) and position 1 of PAM2-C (F76). It should be noted that residues F76, V77, and P78 play different roles in these structures; they bind to the N-pocket as a part of PAM2-N and to the C-pocket as a part of PAM2-C, providing a structural basis for the prevention of simultaneous binding of two PABC molecules.

eRF3 interaction with PABPC1 multimers on poly(A)

We further investigated whether the eRF3–PABC interaction characterized by ITC and NMR can be extrapolated to the interaction of eRF3 with PABPC1 multimers on the poly(A) tail. We performed the ITC experiments by injecting eRF3a(64–94) into full-length human PABPC1 in the presence or absence of poly(A). We used commercially available poly(A) that was 1000 nt long on average (GE Healthcare, hereafter referred to as A_{1000}), on which more than 10 PABPC1 molecules can multimerize (Gorlach et al. 1994). We confirmed there was no heat exchange during injection of eRF3a(64–94) into the buffer or A_{1000} solution.

The ITC isotherms are shown in Figure 7, and the binding stoichiometry and K_d values obtained by fitting of the titration curve are summarized in Table 3. The binding stoichiometry values were ~0.5 for all ITC results, regardless of the presence or absence of poly(A), indicating that multimerization of PABPC1 on poly(A) does not affect the binding stoichiometry. All PABPC1 molecules in multimers on poly(A) bind to eRF3, as does PABPC1 in the absence of poly(A). The value of 0.5 indicates that ~50% of PABPC1 molecules are not active for eRF3 binding, probably due to aggregation and/or instability of PABPC1 during nucleic acid–free preparation.

Interestingly, PABPC1 affinity increased 100-fold and fivefold for eRF3a(64–94) and F85A in a poly(A)-dependent manner. This is partly due to the increased local concentration of PABPC1 on poly(A), which enhances rebinding of eRF3 to PABPC1. The affinity enhancement for eRF3a(64–94) is remarkably higher than the F85A mutant, suggesting that PAM2-C, which is inactivated in the F85A mutant, also contributes to the rebinding to the PABPC1 multimer on poly(A).

DISCUSSION

We have proposed that in human cells, translation termination-coupled deadenylation is mediated by the termination complex eRF1–eRF3 (Funakoshi et al. 2007). We demonstrated that eRF1–eRF3 competes with the deadenylase complexes Caf1–Ccr4 and Pan2–Pan3 via interaction of the PAM2 motifs and PABC of PABPC1 (Fig. 8A). Thus, upon translational termination, recruitment of PABPC1-associated eRF1–eRF3 to the ribosomes permits access of the deadenylase complexes to the 3′ end of poly(A), thus coupling up-regulation of deadenylase complex activity and translation termination (Fig. 8B; Ruan et al. 2010).

Among the PAM2-containing proteins (eRF3, Tob, and Pan3), only eRF3 possesses two overlapping motifs. We investigated their biological role by testing the effect of phenylalanine-to-alanine substitutions at PAM2 (position 10) on the rate of deadenylation and mRNA decay, by a dominant-negative approach. We prepared single mutants of eRF3b, namely, F66A and F75A, and the double mutant F66A/F75A, which are supposed to inactivate the PABC-binding affinities of PAM2-N, C, and both motifs, respectively. Overexpression of any of these mutants significantly slowed deadenylation and mRNA decay in comparison to wild-type eRF3b (Fig. 2A,B), suggesting that both PAM2 motifs are required for translation termination-coupled deadenylation. Coimmunoprecipitation demonstrated that overexpression of wild-type eRF3b or F75A excluded endogenous eRF3 from cellular PABPC1, but F66A or F66A/F75A overexpression did not (Fig. 2C), indicating that PAM2-N is critical for PABPC1 binding and that the F75A and other mutants slowed deadenylation by different mechanisms.

Overexpression of F66A or F66A/F76A leaves the endogenous eRF3 molecules on PABPC1 (Fig. 2C), competitively inhibiting access of the deadenylases and slowing deadenylation. Endogenous eRF3 in the translation termination complex is replaced by the overexpressed mutants, which function normally in the translation termination process (Supplemental Fig. 2).

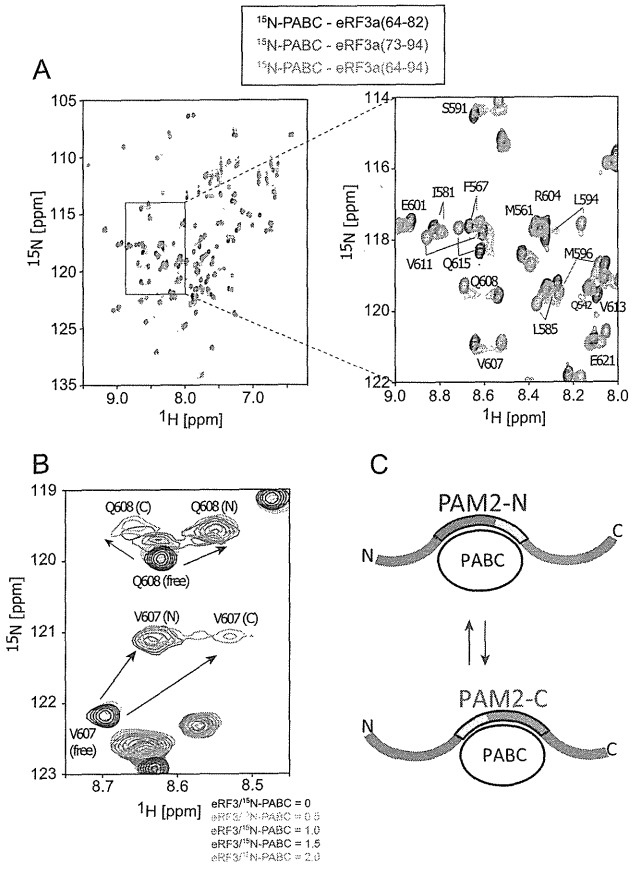

FIGURE 5. Binding of eRF3 to PABC with chemical exchange between complexes PABC–PAM2-N and PABC–PAM2-C. (*A*) Spectral overlay of ^{1}H–^{15}N HSQC of ^{15}N-labeled PABC in the presence of eRF3a fragments. Spectra in the presence of eRF3a fragments, residues 64–82 (black), 73–94 (red), and 64–94 (green). (*B*) Spectral changes of ^{1}H–^{15}N HSQC of ^{15}N-labeled PABC upon sequential additions of eRF3a (64–94). The molar ratios are indicated. (*C*) Schematic drawing of the chemical exchange between complexes PABC–PAM2-N and PABC–PAM2-C. PAM2-N (purple); PAM2-C (red); the overlapping regions (yellow).

On the other hand, overexpression of F75A excluded endogenous eRF3 from PABPC1 as the wild type did, but suppressed deadenylation and mRNA decay (Fig. 2). These results strongly suggest that PAM2-C is required for full activity of eRF3 on deadenylation and mRNA decay.

Although PAM2-C was unable to exclude endogenous eRF3 from cellular PABPC1, as demonstrated by the F66A mutants (Fig. 2C), ITC and NMR analyses demonstrated that PAM2-C also possesses binding affinity for PABC that is 3.5-fold weaker than that of PAM2-N (Table 1). Only one PAM2 motif binds to PABC at a time; PABC in complex with PAM2-N or PAM2-C of eRF3 exchange with each other at an estimated rate of 10^2/sec (Fig. 5). The reported crystal structures (Kozlov and Gehring 2010) and our solution structures of the exchanging complexes (Fig. 6) showed that the overlapping region (residues F76, V77, and P78 in eRF3a) plays a different role in each complex, where the region binds to PABC helices α2 and α3 as a part of PAM2-N, and to helices α3 and α5 as a part of PAM2-C.

We further investigated the interaction of eRF3 with poly(A)-bound PABPC1 multimers (Fig. 7). The stoichiometry was unchanged upon binding to either poly(A)-bound or free PABPC1 or PABC (Table 3), suggesting that most PABPC1 molecules on poly(A) can bind to eRF3. Interestingly, PABPC1 affinity increased 100-fold and fivefold for eRF3a(64-94) and F85A, respectively, in a poly(A)-dependent manner. These results suggest that when multiple PABPC1 molecules are accumulated on poly(A), rebinding of eRF3 to PABPC1 is enhanced. The remarkable 100-fold enhancement of eRF3a(64–94), which contains two overlapping PAM2 motifs, versus fivefold enhancement for the F85A mutant that inactivates PAM2-C, strongly suggests that PAM2-C contributes to rebinding. Since enhanced affinity is observed only when the local PABPC1 concentration increases on poly(A), rebinding to the neighboring molecules of PABPC1 on poly(A) should occur; i.e., eRF3 seems to translocate multiple PABPC1 molecules on poly(A). Therefore, the overlapping PAM2 motifs not only increase affinity for the multimerized PABPC1 but also enable eRF3 to translocate among multiple PABPC1 molecules on poly(A).

This unique interaction mode seems to explain the biological role of the overlapping PAM2 motifs. Tighter binding to the multimerized PABPC1 on poly(A) is beneficial to preclude access of the deadenylases. Enhanced rebinding and translocation increase the probability that the PABPC1 molecule at the most 3′ end of poly(A) enters the eRF3-unbound state and becomes available for the deadenylase complexes (Fig. 8B) when one of the PABPC1-bound

TABLE 2. NMR and refinement statistics for protein structures

	PABC–PAM2-N	PABC–PAM2-C
NMR distance and dihedral constraints		
Distance constraints		
Total NOE	1513	1340
Intra-residue	379	336
Inter-residue		
Sequential ($\|i - j\| = 1$)	412	425
Medium range ($\|i - j\| < 4$)	367	328
Long range ($\|i - j\| > 5$)	290	163
Intermolecular	65	88
Hydrogen bonds	62	62
Total dihedral angle restraints		
Φ	71	59
Structure statistics		
Average pairwise RMSD[a] (Å)		
Heavy	0.80 ± 0.05	0.91 ± 0.05
Backbone	0.34 ± 0.06	0.53 ± 0.05

[a]Pairwise RMSD values were calculated among 20 refined structures, using residues 545–615 of PABPC1 and 68–76 of eRF3a for PABC–PAM2-N, and residues 545–615 of PABPC1 and 76–86 of eRF3a for PABC–PAM2-C.

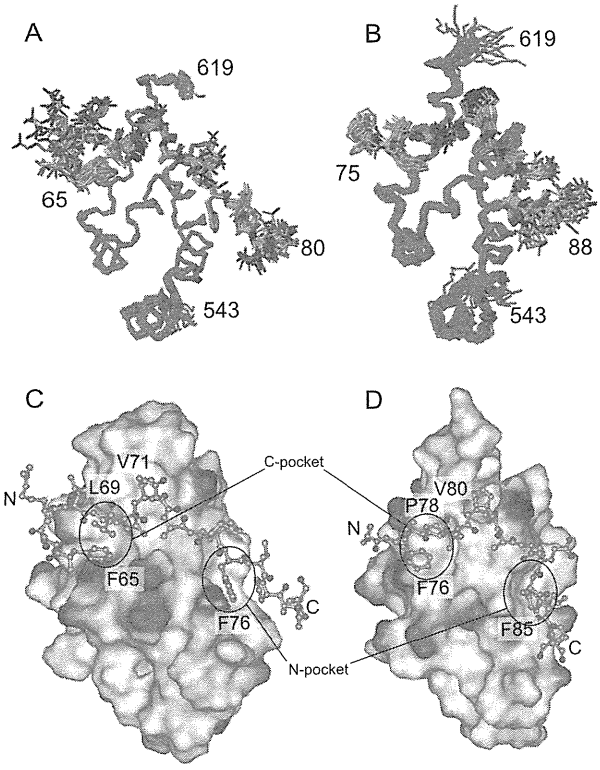

FIGURE 6. Overlay of the 20 structures of (*A*) PABC–eRF3a(64–82), PDB code 2rqg (BMRB code 10019), and (*B*) PABC–eRF3a(73–94), PDB code 2rgh (BMRB code 7033). (*A,B*) Backbone structures of the PABC residues 543–619 (green). Heavy atoms of eRF3a residues 65–80 and 75–88 are shown in *A* and *B*. Residue numbers for both termini are indicated. (*C,D*) Molecular surfaces of PABC, colored by the electrostatic potential, are shown with a ball-and-stick model of the bound eRF3a residues 65–80 (*C*) and 75–88 (*D*). The hydrophobic pockets on PABC (N- and C-pockets) are indicated by ovals.

termination complexes is recruited to the ribosome upon translation termination (Fig. 8C). This allows the up-regulation of deadenylase catalytic activity (Fig. 8B). We propose that this is the molecular mechanism of translation termination-coupled deadenylation, achieved by interaction of overlapping PAM2 motifs with multimerized PABPC1 on poly(A).

MATERIALS AND METHODS

Plasmids

pcDNA6-T7-TR was generated by inverse PCR using pcDNA6/TR (Invitrogen) and the primer pair 5′-CGGCGGCCAGCAGATGG GCTCTAGATTAGATAAAAGTAAAGTG-3′ (sense) and 5′-GTC ATGCTGGCCATGGTGGCCAATTCTTTGCCAAAATGATGAG-3′ (antisense). To construct pCMV-5xMyc-eRF3b, cDNA encoding mouse eRF3b was inserted into the EcoRI and XhoI sites of pCMV-5xMyc (Hosoda et al. 2011). pCMV-5xMyc-eRF3b mutants were generated by converting TTC (F66, F75) to GCC (Ala) using the QuikChange® Site-Directed Mutagenesis Kit (Stratagene).

Immunoprecipitation

HeLa cells were lysed in buffer A (20 mM Tris-HCl at pH 7.5, 50 mM NaCl, 2.5 mM EDTA, 0.5% Nonidet P-40, 0.1 mM PMSF, 2 μg/mL aprotinin, 2 μg/mL leupeptin, and 1 μg/mL RNase A) for 30 min at 4°C. After centrifugation at 15,000*g* for 10 min, the supernatant was incubated with anti-PABPC1 or preimmune serum and Protein A Sepharose 4 Fast Flow (GE Healthcare). The resin was washed three times with buffer A. Bound protein was eluted with SDS-PAGE sample buffer and analyzed by Western blotting using anti-PABPC1, anti-Myc, or anti-eRF3.

Transcriptional pulse-chase analysis

HeLa cells were cotransfected with the pFlag-CMV5/TO-Gl (Funakoshi et al. 2007) reporter plasmid, pCMV-5xFlag-EGFP reference plasmid (Hosoda et al. 2011), pcDNA6-T7-TR repressor plasmid, and either pCMV-5xMyc, pCMV-5xMyc-eRF3b, pCMV-5xMyc-eRF3b (F66A), pCMV-5xMyc-eRF3b (F75A), or pCMV-5xMyc-eRF3b (F66A/F75A). After 24 h, cells were treated with 10 ng/mL tetracycline for 2.5 h to induce transcription, washed three times with phosphate-buffered saline to remove the tetracycline, and harvested after transcription shut-off. Total RNA was isolated as described previously (Funakoshi et al. 2007). To analyze deadenylated mRNA, 20 μg of total RNA was incubated with RNase H and oligo(dT)$_{20}$, as described previously (Hosoda et al. 2011). 5xFlag-EGFP and Flag-β-globin mRNAs were detected by Northern blotting using [^{32}P]-labeled oligonucleotides: 5′-CTCCTCAGGAGT CAGGTGCACCAT-3′, 5′-GGTCCAAGGGTAGACCACCAGCAG-3′, and 5′-CTTATCGTCGTCATCCTTGTAATC-3′. The average length of poly(A) tails at each time point was calculated by auto peak search analysis using Image Gauge Ver. 4.23 (FUJIFILM) software. The half-life of Flag-β-globin mRNA, which was normalized by 5xFlag-EGFP mRNA, was determined by measuring the intensity of the radioactive band with Image Gauge Ver. 4.23 (FUJIFILM) software.

Protein expression and purification

The N-terminal domain of eRF3a (residues 1–207), PABC (residues 541–623 of human PABPC1), and full-length human PABPC1 were expressed as glutathione *S*-transferase (GST)-fusion proteins in BL21(DE3) (Invitrogen) *Escherichia coli*, using the vector pET-42b (Novagen). Other fragments of eRF3a (residues 51–102, 64–94, 64–82, and 79–94) and three mutants of eRF3a (residues 64–94), F76A, F85A, and F76A/F85A, were also expressed as GST-fusion proteins, using the vector pGEX-6P1 (GE Healthcare). The GST-fusion proteins were purified on a Glutathione-Sepharose 4B column (GE Healthcare), followed by digestion with factor Xa (Novagen) or PreScission Protease (GE Healthcare). The cleaved GST and the uncleaved fusion proteins were removed by chromatography on a Glutathione-Sepharose 4B column. Further purification using a reverse-phase C_{18} column was carried out for the eRF3a fragments (residues 51–102, 64–94, and 64–82), and the three mutants of eRF3a (residues 64–94) and PABC. For full-length PABPC1, bound nucleotides were removed by a poly(U)-Sepharose column followed by a MonoS column to remove partially digested PABPC1. The molecular weights of all eRF3 fragments and PABC were confirmed using matrix-assisted laser desorption/ionization mass spectroscopy. These proteins were lyophilized and dialyzed against the buffer used for each analysis. PABC refolded upon

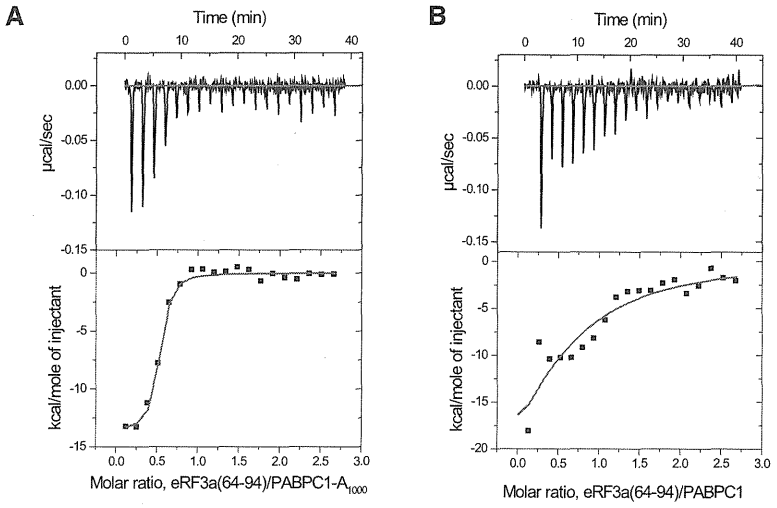

FIGURE 7. Isothermal titration microcalorimetric analyses of the interactions between eRF3a(64–94) and full-length PABPC1. (*Upper* panels) Trace of the calorimetric titration of 19 2-µL aliquots of eRF3a(64–94) into the cell containing PABPC1 in the presence (*A*) or absence (*B*) of A_{1000}. (*Lower* panels) The integrated binding isotherm obtained from the experiment was fitted using a single-site model. Parameters obtained from the best fit (solid line) with error values calculated from the fittings are summarized in Table 3.

dissolving in the buffer, which was confirmed by the chemical shift dispersion of the ^{1}H-NMR spectra. Four eRF3a peptides, for residues 64–75, 64–78, 73–94, and 76–94, were synthesized by QIAGEN K.K. A 37-residue peptide consisting of residues 64–81, followed by residues 76–94, was synthesized by Funakoshi Co., Ltd. Hereafter, we refer to the eRF3a fragment peptide consisting of the residues *x* to *y* as eRF3a(*x*–*y*).

Isothermal titration calorimetry

Binding of eRF3a fragments to PABC and of eRF3a(64–94) to full-length PABPC1 were measured by isothermal titration calorimetry (ITC) (Wiseman et al. 1989) using a MicroCal VP-ITC or iTC200 MicroCalorimeter (MicroCal Inc.). Protein samples were dialyzed against a buffer containing 10 mM Tris-HCl (pH 7.4) and 1 mM dithiothreitol. Experiments were performed at 25°C. PABC (20–50 µM) was titrated with different eRF3a fragments (0.2–0.5 mM), or a fixed amount of PABPC1 (4.5 µM) was titrated with eRF3a(64–94) or its F85A derivative (58 µM). Poly(A) (A_{1000}) was dialyzed to remove shorter fragments of poly(A), and the length was examined by agarose gel electrophoresis. Then, A_{1000} was quantified based on the extinction coefficient of 16 or 24 bases of poly(A) tract (A_{16} or A_{24}), and mixed with PABPC1 at a concentration corresponding to 4.5 µM A_{16} or A_{24}. Heats of dilution were determined by titration into the dialysis buffer and were subtracted from the raw titration data before analysis, using the MicroCal Origin software version 5.0, provided by the manufacturer. A single-site binding model was assumed. The thermodynamic parameters with error values were calculated from the fittings.

NMR spectroscopy

NMR samples were prepared at 0.5–1.0 mM in 95% H_2O, 5% ^2H_2O buffer (20 mM K_2HPO_4, 150 mM NaCl at pH 6.7). NMR spectra were recorded at 30°C on a Bruker Avance 600 spectrometer, equipped with a triple axis gradient probe. Titrations of the ^{15}N-labeled PABC with unlabeled eRF3 fragments or ^{15}N-labeled eRF3 fragments with unlabeled PABC were monitored by ^{1}H–^{15}N HSQC spectra. NMR data processing and analysis were performed using XwinNMR (Bruker A.G.) and Sparky (T.D. Goddard and D.G. Kneller, SPARKY 3, University of California, San Francisco).

PABC in complex with eRF3a(64–82), containing PAM2-N with a GPLGS sequence at its N terminus, and PABC in complex with eRF3a(76–94) containing PAM2-C were prepared at a stoichiometry of 1:1. For heteronuclear NMR experiments, ^{13}C,^{15}N-labeled PABC–eRF3a(64–82); ^{13}C,^{15}N-labeled PABC–eRF3a(79–94); and PABC–^{15}N-labeled eRF3a(64–82) were prepared.

Sequential assignments of the backbone resonances of PABC were achieved by HNCACB, CBCA(CO)NH, HBHANH, HBHA(CBCACO)NH, ^{15}N-edited TOCSY-HSQC, and ^{15}N-edited NOESY-HSQC experiments. Side-chain assignments were obtained from H(CCO)NH, C(CO)NH, and HCCH-TOCSY experiments. Stereospecific assignments of the valine and leucine methyl groups of PABC were obtained by analyzing constant time ^{1}H–^{13}C HSQC spectra of 10% ^{13}C-enriched PABC complexed with eRF3a(64–82) and eRF3a(79–94), respectively (Neri et al. 1989).

Assignments of the ^{15}N-labeled eRF3a(64–82) of eRF3a in complex with PABC were carried out by analyzing ^{15}N-edited NOESY-HSQC and ^{15}N-edited TOCSY-HSQC, while assignments of eRF3a(79–94) in complex with ^{13}C,^{15}N-labeled PABC were based on NOE connectivities by analyzing a series of isotope filter experiments using [^{13}C,^{15}N/F2]-filtered NOESY and TOCSY, [^{13}C/F1,F2]-filtered NOESY.

Structure calculation

Approximate interproton distances were obtained from ^{13}C-edited NOESY-HSQC, ^{15}N-edited NOESY-HSQC, [^{13}C/F_3]-filtered [^{13}C/F_1]-edited HMQC-NOESY, and isotope-filtered NOESY spectra. The mixing time was 150 msec for all NOESY experiments.

The backbone coupling constants $^3J_{NH\alpha}$ were measured from an HNHA experiment. The φ dihedral angle restraints were derived from the $^3J_{NH\alpha}$ coupling constants and the chemical shift

TABLE 3. Binding stoichiometry and dissociation constant values for interaction of eRF3a(64–94) and its mutant derivative with PABPC1

eRF3a residues	PABPC1-A_{1000} or PABPC1	Binding stoichiometry (eRF3/PABPC1)	K_d (µM)
64–94	PABPC1-A_{1000}	0.49 ± 0.01	0.04 ± 0.01
64–94	PABPC1	0.5 ± 0.5	4 ± 3
64–94(F85A)	PABPC1-A_{1000}	0.41 ± 0.04	0.6 ± 0.1
64–94(F85A)	PABPC1	0.5 (fixed)[a]	3.1 ± 0.4

[a]Binding stoichiometry was fixed at 0.5 during fitting.

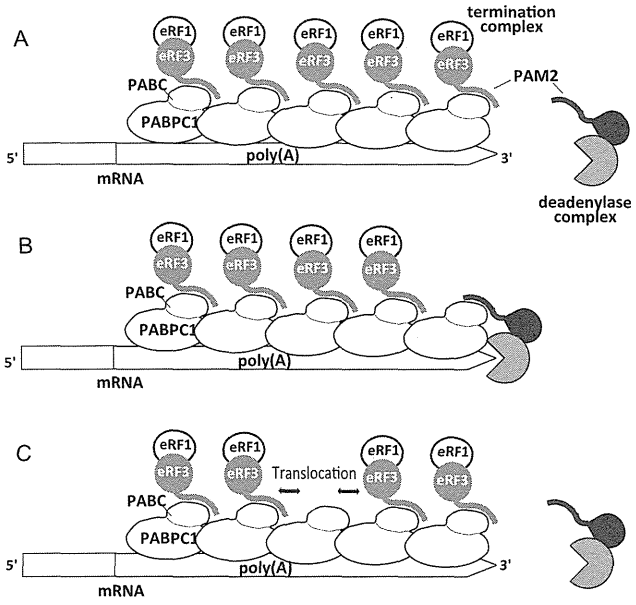

FIGURE 8. Schematic drawing of the translation termination-coupled regulation of the PAM2-containing deadenylase complexes by eRF3. (*A*) Competitive suppression of deadenylase activity by eRF3 binding to PABPC1. (*B*) Activation of PAM2-containing deadenylases through the dual interactions of PAM2–PABC and deadenylase–poly(A). (*C*) Possible role of the overlapping PAM2 motifs in eRF3. Upon the recruitment of one of the eRF3 molecules to the ribosome, relocation of eRF3 among the poly(A)-bound PABPC1 molecules would eventually allow a particular PABPC1 to become available for the dual deadenylase interactions, as shown in *B*.

indices. Values of $-60° \pm 30°$ were used for the φ dihedral angles for α-helical regions.

A series of ^{1}H–^{15}N HSQC spectra was acquired on a sample freshly dissolved in $^{2}H_2O$ to identify the slowly exchanging amides. Amides that had not exchanged after 1 h and were located in regions with defined secondary structure based on NOE data were restrained to form HN–CO hydrogen bonds using the distance restraints $d_{O\text{-}N}$ = 3.3 Å and $d_{O\text{-}HN}$ = 2.3 Å.

CYANA version 2.1 (Guntert 2004; Nederveen et al. 2005) was used to compute seven cycles, each with 600 structures. The input data and structure calculation statistics are summarized in Table 2. The accuracy of the NMR models may be assessed based on the criteria for successful structure calculation using the program CYANA, as defined by Jee and Guntert (2003). The 20 lowest-energy (total energy) structures were chosen for the final structural ensemble. The Ramachandran plots of the final 20 structures, calculated for PABC in complex with eRF3a(64–82) and eRF3a(79–94) using PROCHECK version 3.4.4, showed 76.0% and 81.4%, 22.9% and 18.2%, 1.1% and 0.2%, and 0.0% and 0.2% of the residues in the most favored, additionally allowed, generously allowed, and disallowed regions, respectively (Laskowski et al. 1996).

DATA DEPOSITION

The ^{1}H, ^{13}C, and ^{15}N resonance assignments have been deposited in the BioMagResBank with accession numbers 10019 and 7033 for PABC–eRF3a(64–82) and PABC–eRF3a(79–94), respectively. The structures of the PABC–eRF3a(64–82) and PABC–eRF3a(79–94) complexes have been deposited in the Protein Data Bank with accession codes 2rqg and 2rqh.

SUPPLEMENTAL MATERIAL

Supplemental material is available for this article.

ACKNOWLEDGMENTS

This work was supported in part by grants from the Japan New Energy and Industrial Technology Development Organization (NEDO) and the Ministry of Economy, Trade, and Industry (METI) (to I.S.); a Grant-in-Aid for Scientific Research on Priority Areas from the Japanese Ministry of Education, Culture, Sports, Science, and Technology (to M.O. and I.S.); and a grant from the Takeda Science Foundation (to M.O.).

Received June 29, 2012; accepted July 31, 2012.

REFERENCES

Albrecht M, Lengauer T. 2004. Survey on the PABC recognition motif PAM2. *Biochem Biophys Res Commun* **316:** 129–138.

Bianchin C, Mauxion F, Sentis S, Seraphin B, Corbo L. 2005. Conservation of the deadenylase activity of proteins of the Caf1 family in human. *RNA* **11:** 487–494.

Cavanagh J, Fairbrother WJ, Palmer AG III, Rance M, Skelton NJ. 2006. Chemical exchange effects in NMR spectroscopy. In *Protein NMR spectroscopy principles and practice*, 2nd ed., pp. 391–404. Elsevier Academic Press, Burlington, MA.

Chen J, Chiang YC, Denis CL. 2002. CCR4, a 3′–5′ poly(A) RNA and ssDNA exonuclease, is the catalytic component of the cytoplasmic deadenylase. *EMBO J* **21:** 1414–1426.

Cosson B, Couturier A, Chabelskaya S, Kiktev D, Inge-Vechtomov S, Philippe M, Zhouravleva G. 2002. Poly(A)-binding protein acts in translation termination via eukaryotic release factor 3 interaction and does not influence [*PSI*$^{+}$] propagation. *Mol Cell Biol* **22:** 3301–3315.

Daugeron MC, Mauxion F, Seraphin B. 2001. The yeast *POP2* gene encodes a nuclease involved in mRNA deadenylation. *Nucleic Acids Res* **29:** 2448–2455.

Decker CJ, Parker R. 1993. A turnover pathway for both stable and unstable mRNAs in yeast: Evidence for a requirement for deadenylation. *Genes Dev* **7:** 1632–1643.

Ezzeddine N, Chang TC, Zhu W, Yamashita A, Chen CY, Zhong Z, Yamashita Y, Zheng D, Shyu AB. 2007. Human TOB, an antiproliferative transcription factor, is a poly(A)-binding protein-dependent positive regulator of cytoplasmic mRNA deadenylation. *Mol Cell Biol* **27:** 7791–7801.

Fritz DT, Bergman N, Kilpatrick WJ, Wilusz CJ, Wilusz J. 2004. Messenger RNA decay in mammalian cells: The exonuclease perspective. *Cell Biochem Biophys* **41:** 265–278.

Frolova L, Le Goff X, Rasmussen HH, Cheperegin S, Drugeon G, Kress M, Arman I, Haenni AL, Celis JE, Philippe M, et al. 1994. A highly conserved eukaryotic protein family possessing properties of polypeptide chain release factor. *Nature* **372:** 701–703.

Funakoshi Y, Doi Y, Hosoda N, Uchida N, Osawa M, Shimada I, Tsujimoto M, Suzuki T, Katada T, Hoshino S. 2007. Mechanism of mRNA deadenylation: Evidence for a molecular interplay between translation termination factor eRF3 and mRNA deadenylases. *Genes Dev* **21:** 3135–3148.

Gorlach M, Burd CG, Dreyfuss G. 1994. The mRNA poly(A)-binding protein: Localization, abundance, and RNA-binding specificity. *Exp Cell Res* **211:** 400–407.

Guntert P. 2004. Automated NMR structure calculation with CYANA. *Methods Mol Biol* **278:** 353–378.

Hoshino S, Hosoda N, Araki Y, Kobayashi T, Uchida N, Funakoshi Y, Katada T. 1999a. Novel function of the eukaryotic polypeptide-chain releasing factor 3 (eRF3/GSPT) in the mRNA degradation pathway. *Biochemistry (Mosc)* **64:** 1367–1372.

Hoshino S, Imai M, Kobayashi T, Uchida N, Katada T. 1999b. The eukaryotic polypeptide chain releasing factor (eRF3/GSPT) carrying the translation termination signal to the 3′-poly(A) tail of mRNA. Direct association of erf3/GSPT with polyadenylate-binding protein. *J Biol Chem* **274:** 16677–16680.

Hosoda N, Kobayashi T, Uchida N, Funakoshi Y, Kikuchi Y, Hoshino S, Katada T. 2003. Translation termination factor eRF3 mediates mRNA decay through the regulation of deadenylation. *J Biol Chem* **278:** 38287–38291.

Hosoda N, Funakoshi Y, Hirasawa M, Yamagishi R, Asano Y, Miyagawa R, Ogami K, Tsujimoto M, Hoshino S. 2011. Anti-proliferative protein Tob negatively regulates CPEB3 target by recruiting Caf1 deadenylase. *EMBO J* **30:** 1311–1323.

Ikematsu N, Yoshida Y, Kawamura-Tsuzuku J, Ohsugi M, Onda M, Hirai M, Fujimoto J, Yamamoto T. 1999. Tob2, a novel anti-proliferative Tob/BTG1 family member, associates with a component of the CCR4 transcriptional regulatory complex capable of binding cyclin-dependent kinases. *Oncogene* **18:** 7432–7441.

Jee J, Guntert P. 2003. Influence of the completeness of chemical shift assignments on NMR structures obtained with automated NOE assignment. *J Struct Funct Genomics* **4:** 179–189.

Jia S, Meng A. 2007. Tob genes in development and homeostasis. *Dev Dyn* **236:** 913–921.

Kononenko AV, Mitkevich VA, Atkinson GC, Tenson T, Dubovaya VI, Frolova LY, Makarov AA, Hauryliuk V. 2010. GTP-dependent structural rearrangement of the eRF1:eRF3 complex and eRF3 sequence motifs essential for PABP binding. *Nucleic Acids Res* **38:** 548–558.

Kozlov G, Gehring K. 2010. Molecular basis of eRF3 recognition by the MLLE domain of poly(A)-binding protein. *PLoS ONE* **5:** e10169. doi: 10.1371/journal.pone.0010169.

Kozlov G, Trempe JF, Khaleghpour K, Kahvejian A, Ekiel I, Gehring K. 2001. Structure and function of the C-terminal PABC domain of human poly(A)-binding protein. *Proc Natl Acad Sci* **98:** 4409–4413.

Kozlov G, Siddiqui N, Coillet-Matillon S, Trempe JF, Ekiel I, Sprules T, Gehring K. 2002. Solution structure of the orphan PABC domain from *Saccharomyces cerevisiae* poly(A)-binding protein. *J Biol Chem* **277:** 22822–22828.

Kozlov G, De Crescenzo G, Lim NS, Siddiqui N, Fantus D, Kahvejian A, Trempe JF, Elias D, Ekiel I, Sonenberg N, et al. 2004. Structural basis of ligand recognition by PABC, a highly specific peptide-binding domain found in poly(A)-binding protein and a HECT ubiquitin ligase. *EMBO J* **23:** 272–281.

Kozlov G, Menade M, Rosenauer A, Nguyen L, Gehring K. 2010. Molecular determinants of PAM2 recognition by the MLLE domain of poly(A)-binding protein. *J Mol Biol* **397:** 397–407.

Laskowski RA, Rullmannn JA, MacArthur MW, Kaptein R, Thornton JM. 1996. AQUA and PROCHECK-NMR: Programs for checking the quality of protein structures solved by NMR. *J Biol NMR* **8:** 477–486.

Mauxion F, Chen CY, Seraphin B, Shyu AB. 2009. BTG/TOB factors impact deadenylases. *Trends Biochem Sci* **34:** 640–647.

Meyer S, Temme C, Wahle E. 2004. Messenger RNA turnover in eukaryotes: Pathways and enzymes. *Crit Rev Biochem Mol Biol* **39:** 197–216.

Nederveen AJ, Doreleijers JF, Vranken W, Miller Z, Spronk CA, Nabuurs SB, Guntert P, Livny M, Markley JL, Nilges M, et al. 2005. RECOORD: A recalculated coordinate database of 500+ proteins from the PDB using restraints from the BioMagResBank. *Proteins* **59:** 662–672.

Neri D, Szyperski T, Otting G, Senn H, Wuthrich K. 1989. Stereospecific nuclear magnetic resonance assignments of the methyl groups of valine and leucine in the DNA-binding domain of the 434 repressor by biosynthetically directed fractional ^{13}C labeling. *Biochemistry* **28:** 7510–7516.

Parker R, Song H. 2004. The enzymes and control of eukaryotic mRNA turnover. *Nat Struct Mol Biol* **11:** 121–127.

Prevot D, Morel AP, Voeltzel T, Rostan MC, Rimokh R, Magaud JP, Corbo L. 2001. Relationships of the antiproliferative proteins BTG1 and BTG2 with CAF1, the human homolog of a component of the yeast CCR4 transcriptional complex: Involvement in estrogen receptor α signaling pathway. *J Biol Chem* **276:** 9640–9648.

Roy G, De Crescenzo G, Khaleghpour K, Kahvejian A, O'Connor-McCourt M, Sonenberg N. 2002. Paip1 interacts with poly(A) binding protein through two independent binding motifs. *Mol Cell Biol* **22:** 3769–3782.

Ruan L, Osawa M, Hosoda N, Imai S, Machiyama A, Katada T, Hoshino SI, Shimada I. 2010. Quantitative characterization of Tob interactions provides the thermodynamic basis for translation termination-coupled deadenylase regulation. *J Biol Chem* **285:** 27624–27631.

Sachs AB, Deardorff JA. 1992. Translation initiation requires the PAB-dependent poly(A) ribonuclease in yeast. *Cell* **70:** 961–973.

Siddiqui N, Mangus DA, Chang TC, Palermino JM, Shyu AB, Gehring K. 2007. Poly(A) nuclease interacts with the C-terminal domain of polyadenylate-binding protein domain from poly(A)-binding protein. *J Biol Chem* **282:** 25067–25075.

Tirone F. 2001. The gene $PC3^{TIS21/BTG2}$, prototype member of the PC3/BTG/TOB family: Regulator in control of cell growth, differentiation, and DNA repair? *J Cell Physiol* **187:** 155–165.

Tucker M, Valencia-Sanchez MA, Staples RR, Chen J, Denis CL, Parker R. 2001. The transcription factor associated Ccr4 and Caf1 proteins are components of the major cytoplasmic mRNA deadenylase in *Saccharomyces cerevisiae*. *Cell* **104:** 377–386.

Uchida N, Hoshino S, Imataka H, Sonenberg N, Katada T. 2002. A novel role of the mammalian GSPT/eRF3 associating with poly(A)-binding protein in Cap/poly(A)-dependent translation. *J Biol Chem* **277:** 50286–50292.

Uchida N, Hoshino S, Katada T. 2004. Identification of a human cytoplasmic poly(A) nuclease complex stimulated by poly(A)-binding protein. *J Biol Chem* **279:** 1383–1391.

Wiseman T, Williston S, Brandts JF, Lin LN. 1989. Rapid measurement of binding constants and heats of binding using a new titration calorimeter. *Anal Biochem* **179:** 131–137.

Yamashita A, Chang TC, Yamashita Y, Zhu W, Zhong Z, Chen CY, Shyu AB. 2005. Concerted action of poly(A) nucleases and decapping enzyme in mammalian mRNA turnover. *Nat Struct Mol Biol* **12:** 1054–1063.

Yoshida Y, Hosoda E, Nakamura T, Yamamoto T. 2001. Association of ANA, a member of the antiproliferative Tob family proteins, with a Caf1 component of the CCR4 transcriptional regulatory complex. *Jpn J Cancer Res* **92:** 592–596.

Zhouravleva G, Frolova L, Le Goff X, Le Guellec R, Inge-Vechtomov S, Kisselev L, Philippe M. 1995. Termination of translation in eukaryotes is governed by two interacting polypeptide chain release factors, eRF1 and eRF3. *EMBO J* **14:** 4065–4072.

Advanced Review

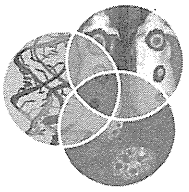

Mechanism of the initiation of mRNA decay: role of eRF3 family G proteins

Shin-ichi Hoshino*

mRNA decay is intimately linked to and regulated by translation in eukaryotes. However, it has remained unclear exactly how mRNA decay is linked to translation. Progress has been made in recent years in understanding the molecular mechanisms of the link between translation and mRNA decay. It has become clear that the eRF3 family of GTP-binding proteins acts as signal transducers that couple translation to mRNA decay and plays pivotal roles in the regulation of gene expression and mRNA quality control. During translation, the translation termination factor eRF3 in complex with eRF1 recognizes the termination codon which appears at the A site of the terminating ribosome. Depending on whether the termination codon is normal (bona fide) or aberrant (premature), deadenylation-dependent decay or nonsense-mediated mRNA decay (NMD) occurs. mRNA without termination codons and mRNA with the propensity to cause the ribosome to stall are recognized as aberrant by other members of the eRF3 family during translation, and these translational events cause nonstop mRNA decay (NSD) and no-go decay (NGD), respectively. In this review, we focus on how mRNA decay is triggered by translational events and summarize the initiation mechanism for the decay of both normal and aberrant mRNAs.

How to cite this article:
WIREs RNA 2012, 3:743–757. doi: 10.1002/wrna.1133

INTRODUCTION

GTP-binding proteins act as molecular switches that change binding partners between the active GTP-bound state and inactive GDP-bound state.[1] The energy released from the hydrolysis of GTP is used for the conformational switch of G proteins, whereas the energy from ATP hydrolysis is mostly utilized for the chemical reaction itself. Among GTP-binding proteins, the best characterized are the signal-transducing G proteins. Each member of this subfamily converts extracellular signals to intracellular signals, where the GDP-bound form interacts with membrane receptors and the GTP-bound form with the effectors.[2] As illustrated by these proteins, G proteins convert signals and couple two different events. Emerging evidence indicates that eRF3 family G proteins act as signal transducers that couple translation to mRNA decay. First, the text begins with a brief review on the structural and functional characteristics of the eRF3 family G proteins.

eRF3 FAMILY OF GTP-BINDING PROTEINS

The eRF3 family is characterized by the highly conserved translation elongation factor eEF1A-like carboxy-terminal domain and a long amino-terminal domain of around 200 amino acids unique to each family member (Figure 1). The G protein subfamily consists of eRF3a/GSPT1,[3] eRF3b/GSPT2,[4] Hbs1,[5] Ski7,[6] GTPBP1, and GTPBP2.[7] The highly conserved C domain can be further divided into three domains. Domain I contains the consensus motifs G1–G4 conserved among members of the GTPase superfamily.[2] Domains II and III of eRF3 and Hbs1 are demonstrated to adopt a fold similar to the corresponding

The author has declared that no competing interests exist.

*Correspondence to: hoshino@phar.nagoya-cu.ac.jp
Department of Biological Chemistry, Graduate School of Pharmaceutical Sciences, Nagoya City University, Nagoya, Japan

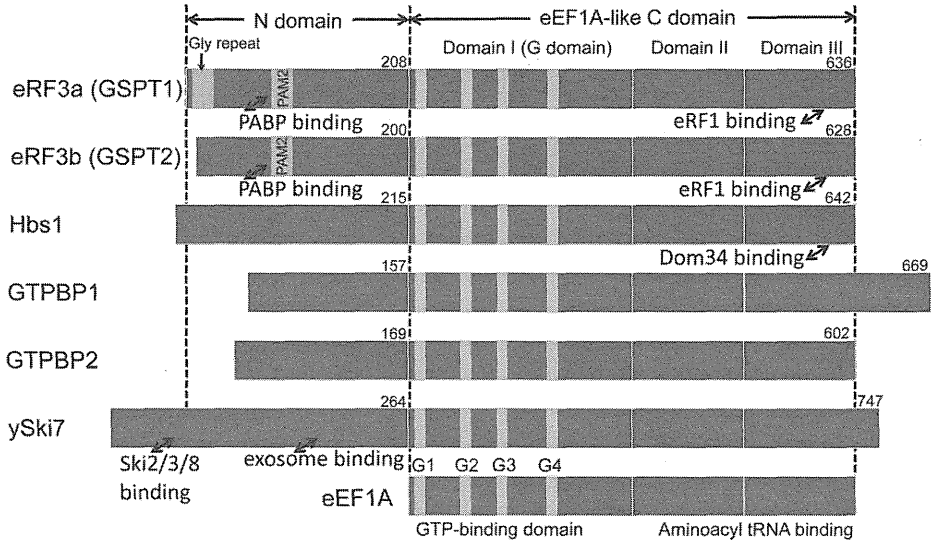

FIGURE 1 | eRF3 family GTP-binding proteins. The family members share a common domain structure, with an amino-terminal domain of ~200 amino acids unique to each member and a carboxy-terminal eEF1A-like structure. Shown are the structures of human eRF3a, eRF3b, Hbs1, GTPBP1, GTPBP2, and yeast Ski7.

domain of eEF1A.[8] Consistent with this, domain III of eRF3 and Hbs1 interacts with the binding partners eRF1 and Dom34, respectively, as eEF1A interacts with tRNA using the corresponding domain.[8] The GTP-bound form of eRF3/Hbs1 preferentially binds to eRF1/Dom34 to form a GTP-eEF1A-tRNA-like structure to enter the ribosomal A site.[9–13] eRF1 recognizes all three stop codons (UAA, UGA, and UAG) at the A site of the ribosome and activates the peptidyl transferase activity of the ribosome to release synthesized polypeptide chains (reviewed in Refs 14 and 15). Dom34 is structurally related to eRF1 but cannot recognize stop codons. Recently, it was shown that Hbs1 and Dom34 enter the A site of an aberrantly stalled ribosome in a codon-nonspecific manner to release peptidyl-tRNA.[16,17] eRF1/Dom34 also contacts GTP-binding domain I of eRF3/Hbs1 and this contact is thought to contribute to the activation of the GTPase activity. Thus, eRF1/Dom34 and the ribosome act as GTPase-activating proteins (GAPs) for eRF3/Hbs1. As suggested by the structural similarities to eEF1A, the functional properties of eEF1A related to the translational regulation appear to be conserved among the eRF3 family members.

However, the eRF3 family has evolved a unique N-terminal domain (NTD), which is not present in eEF1A. Functional roles of the N-domain are well-established in eRF3. The N-domain of eRF3 specifically interacts with poly(A)-binding protein (PABP)[18] to accelerate the next round of translation initiation by efficiently recycling the terminating ribosome[19] (see *Roles of 3′ Terminal Poly(A) Tail of mRNA in Both Translation and mRNA Decay* section) and also to regulate the initiation of mRNA decay (deadenylation).[20,21] Thus, in addition to its role in translation termination, eRF3 regulates termination-coupled events. The N-domain of eRF3 contains PABP-interacting motifs (PAM2) originally identified for Paip1/Paip2[22] and directly interacts with the PABC/MLLE domain of PABP.[12,21,23] The PAM2 motif is not conserved among the other eRF3 family members. On the other hand, the N-domain of Ski7 interacts with the exosome and RNA-binding Ski2/3/8 complex.[24] These interactions are required for the 3′ to 5′ decay of mRNA.[25] eRF3 and Ski7 regulate different steps of mRNA decay: deadenylation and 3′ to 5′ decay of mRNA, respectively (see below for details). Thus eRF3 family G proteins are involved not only in translational regulation but also in mRNA decay.

ROLES OF 3′ TERMINAL POLY(A) TAIL OF mRNA IN BOTH TRANSLATION AND mRNA DECAY

To better understand the mechanism of mRNA decay, next the structure of mRNA is described. In eukaryotes, mRNA is matured by adding the 5′ 7-methylguanosine cap and the 3′ poly(A) tail co-transcriptionally. The two terminal structures interact with a cap-binding protein (initiation factor 4E, eIF4E) and a PABP, respectively. By the interaction of the two proteins indirectly through a scaffold protein

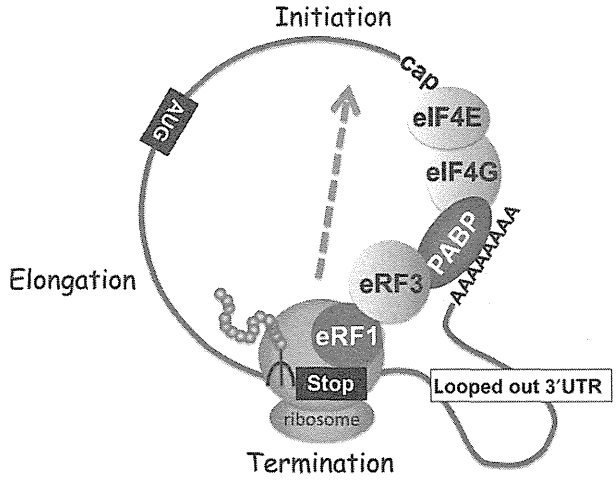

FIGURE 2 | mRNA closed-loop structure. eIF4E bound to the 5′ cap and PABP bound to the 3′ poly(A) tail form a complex with the scaffold protein eIF4G. This leads to the formation of a closed-loop structure of mRNA. The binding of eRF3 to PABP could further loop-out the long 3′ untranslated region of the mRNA and place the termination site in the vicinity of the initiation site, thereby contributing to translation by efficiently recruiting the terminating ribosome to the next round of translation initiation.

eIF4G, mRNA forms a circular structure, which is demonstrated by electron microscopy and atomic force microscopy (Figure 2). Furthermore, because the translation termination factor eRF3 and eIF4G bind to form a complex with PABP,[19] the translation termination site could come into close proximity to the translation initiation site by the looping out of the long 3′ untranslated region (3′UTR). Such a closed-loop structure is thought to contribute to translation by efficiently recruiting/recycling the terminating ribosome to the next round of translation initiation.[19] In fact, the cap and poly(A) tail synergistically stimulate translation in an *in vitro* translation system and *in vivo*.

In addition to its role in translation, the poly(A) tail is also pivotal to mRNA decay. As described in detail in the next section, shortening of the poly(A) tail is the first step of general mRNA decay.[26] After this shortening, the mRNA body is rapidly degraded. It is important to note that the shortening of the poly(A) tail is the rate-limiting step of mRNA decay.[26] Thus, the poly(A) tail plays pivotal roles in the regulation of both translation and mRNA stability. General mRNA with a poly(A) tail is protected against mRNA decay and also subjected to efficient translation.

mRNA DECAY PATHWAY

After transcription, splicing and processing (including capping and polyadenylation), mRNA is matured in the nucleus. At this stage, some of the incorrectly processed transcripts are degraded by nuclear mRNA quality control system (reviewed in Ref 27). Properly processed mature form of mRNA is transported to the cytoplasm where translation occurs (Figure 3). Also, mRNA decay occurs co-translationally.[28–31] The newly synthesized mature mRNA contains ~200 and ~90 bases of the 3′ poly(A) tail in humans and yeast, respectively, and the 3′ poly(A) tail is gradually shortened while translation proceeds. Following the poly(A) tail shortening, removal of the 5′ cap and 5′ to 3′ exonucleolytic degradation occur as the major pathways (reviewed in Ref 32). In some cases, deadenylated mRNA could be transported to cytoplasmic granules called 'P bodies', where mRNA is stored, returned for translation, or degraded.[33]

The mRNA decay pathway in conjunction with the translating ribosome is depicted in Figure 4. As mentioned above, shortening of the poly(A) tail to an oligo(A) form is the first and rate-limiting step of mRNA decay. The shortening, termed deadenylation, is catalyzed by the two major mRNA deadenylase complexes Pan2–Pan3 and Caf1–Ccr4, which are conserved from yeast[34] to humans[35] (Caf1 is also referred to as Pop2). The deadenylation consists of two steps, in which Pan2–Pan3 catalyzes trimming of the long poly(A) tail in the early phase, and Caf1–Ccr4 catalyzes exonucleolytic degradation of shorter poly(A) tails in the late phase of the deadenylation process.[34,35] In yeast, the rate of deadenylation is not affected by the lesions of PAN2 or PAN3, thus Caf1–Ccr4 is thought to be the major mRNA deadenylase responsible for determining the rate of deadenylation.[34]

When the poly(A) tail is shortened to about 10 nucleotides, cleavage of the 5′ cap structure, a process termed decapping, occurs (reviewed in Ref 36). As the minimal size of the poly(A) residues required for the binding of PABP is about 12 nucleotides, PABP is probably released from the mRNA at this time. After PABP is released, mRNA with an oligo(A) tail is the most favorable substrate for the decapping activator Lsm–Pat1 complex, which is composed of the Sm-like RNA-binding proteins Lsm1–Lsm7 and the Pat1 protein.[36] The binding of the Lsm1–7–Pat1 complex to the oligo(A) tail prevents further 3′ to 5′ exonucleolytic degradation by the exosome and acts as a binding platform for the decapping enzyme complex Dcp1–Dcp2 as well as other decapping activators Dhh1/Rck, Edc3, and Hedls. The recruitment of the complex accelerates decapping by the catalytic enzyme Dcp2. As described above, PABP bound to the 3′ end of the poly(A) tail forms a complex with the cap-binding protein eIF4E through interaction with the scaffold protein eIF4G (Figure 2), and the resulting structure helps to stabilize the cap-eIF4E interaction

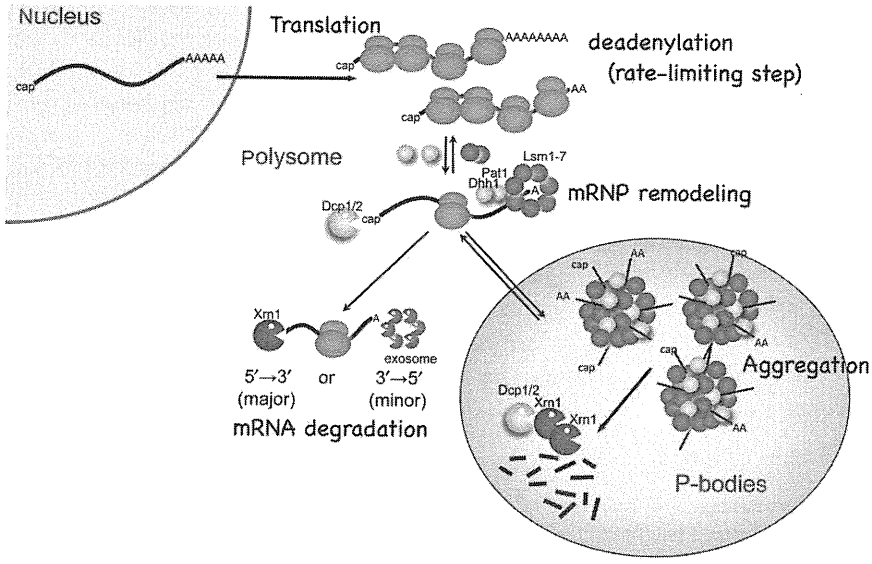

FIGURE 3 | Life-cycle of an mRNA. After transcription, splicing and pre-mRNA processing including capping and polyadenylation in the nucleus, mRNA matures and is transported to the cytoplasm, where translation occurs. mRNA decay also occurs while translation proceeds. In the first step of mRNA decay, the 3′ poly(A) tail is shortened co-translationally. Subsequent processes including decapping and 5′ to 3′ decay of the deadenylated mRNA also occur on the polysome. In some cases, deadenylated mRNA could be transported to cytoplasmic granules called 'P bodies' and be stored, returned for translation or degraded.

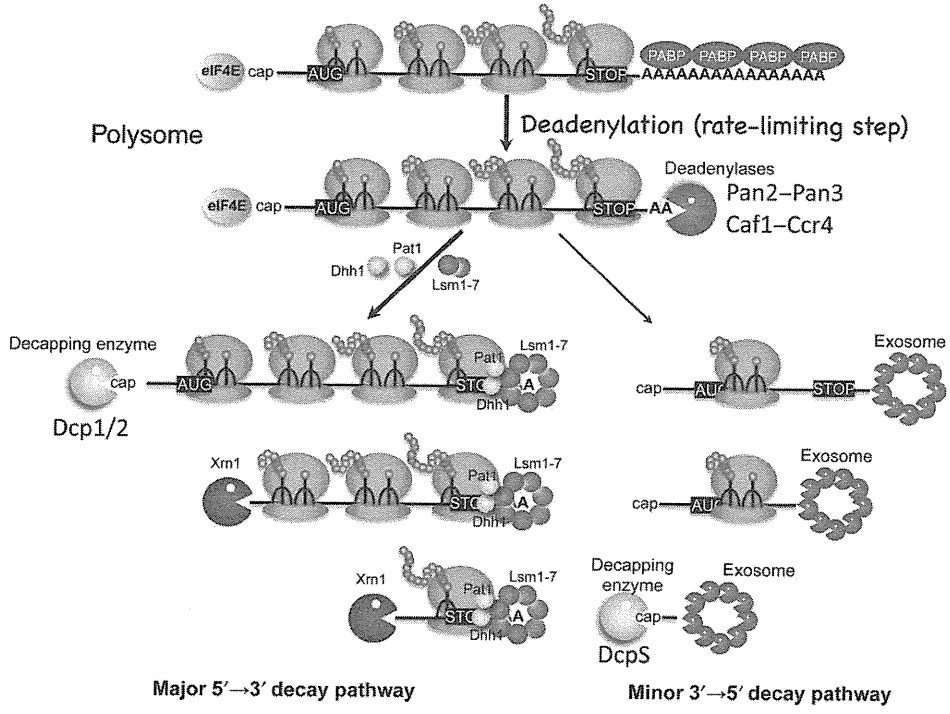

FIGURE 4 | mRNA decay pathway of general mRNA. The first step of mRNA decay is the shortening of the 3′ poly(A) tail. The step called deadenylation is the rate-limiting step of mRNA decay. The two major mRNA deadenylase complexes Pan2–Pan3 and Caf1–Ccr4 sequentially catalyze the reaction. After poly(A) tails are shortened to ~10 nucleotides, decapping activators consisting of Lsm1–7, Dhh1/Rck, Pat1, Edc3, and Hedls etc. bind to the 3′ terminus and recruit the decapping enzyme Dcp1–Dcp2 to the 5′ terminus, which is associated with the 3′ terminus by the formation of a closed-loop structure of the mRNA (Figure 2). The Lsm–Pat1–Dhh1 complex formed at the 3′ terminus blocks exonucleolytic degradation from the 3′ terminus by the exosome, and Xrn1-catalyzed 5′ to 3′ decay proceeds as the major decay pathway. The 5′ to 3′ decay pathway enables even the last translating ribosome to produce a full-length intact protein. Alternatively, a 3′ to 5′ decay pathway is also known.

and to prevent decapping by competing with the interaction with the decapping enzyme. Thus PABP acts as an inhibitor of decapping, and the release of PABP from mRNA triggers release of the eIF4G/4E complex from the 5′ cap and thus enables access by the decapping enzyme. Although it is curious that removal of the 5′ cap occurs after shortening of the 3′ poly(A) tail, it makes sense if we consider the circularized structure of the mRNA (Figure 2).

Pat1 also provides a binding surface for Xrn1, the major enzyme known to catalyze 5′ to 3′ exonucleolytic degradation of mRNA in the cytoplasm, and accelerates degradation of the decapped mRNA. Thus mRNA is degraded mainly in the 5′ to 3′ direction. This 5′ to 3′ directional mRNA decay is reasonable, as in theory the last ribosome to start translation during mRNA decay could complete translation to produce a full-length protein (Figure 4, left pathway). In addition to the 5′ to 3′ pathway, a 3′ to 5′ pathway, which is catalyzed by the exosome, is also known to operate as an alternative pathway.

WHAT IS THE TRIGGER OF mRNA DECAY?

As described above, mRNA is degraded on polysomes co-translationally by a deadenylation-dependent decay pathway. When the poly(A) tail is shortened to about 10 nucleotides, the mRNA body is rapidly degraded in yeast and higher eukaryotes. However, an important question has remained to be determined: what triggers the shortening of the poly(A) tail? It has been found that the translation termination factor eRF3 is involved in triggering shortening of the poly(A) tail.[20,21,37]

In eukaryotes, translation is divided into four steps; initiation, elongation, termination, and ribosome recycling. Translation termination is governed by the two eukaryotic releasing factors eRF1 and eRF3 (reviewed in Refs 14 and 15). When protein synthesis is catalyzed by the ribosome and the final peptide bond is formed, the peptidyl-tRNA is translocated from the A site to the P site in the ribosome and one of the three termination codons (UAA, UGA, or UAG) appears at the A site. The class I release factor eRF1 directly binds to recognize the termination codon and accelerates the release of the synthesized peptide, which is catalyzed by the peptidyl-transferase center of the ribosome. At this time, the class II release factor eRF3 binds to form a complex with eRF1 and recruits eRF1 to the ribosome,[11–13,37] in the same way as the elongation factor eEF1A, which recruits tRNA to the ribosome. Actually, eRF3 is a GTP-binding protein similar to eEF1A, and eRF3 forms a complex with eRF1 and recruits eRF1 to the ribosome in its GTP-bound form.[11–13,37] In turn, the ribosome and eRF1 activate the GTPase activity of eRF3 and the resulting GDP-bound form of eRF3 dissociates from eRF1 and the ribosome. eRF3, as well as eRF1, is essential for translation termination, however, the NTD characteristic of eRF3 is dispensable for the termination reaction. Thus, it is reasonable to think that the NTD is involved in functions other than eEF1A-like translational regulation. Consistent with this idea, the NTD was found to interact with the poly(A)-binding protein PABP,[18,38] which binds specifically to the 3′ terminal poly(A) tail of mRNA. This led to speculation that eRF3 is involved in the regulation of poly(A) tail length.[38]

By using yeast genetics, the effect of eRF3 lesions on the stability of mRNA was examined. Either temperature-sensitive mutation of eRF3, deletion of NTD from eRF3, or overexpression of NTD resulted in the stabilization of mRNA.[20] The defects were also observed in the first step of mRNA decay, the poly(A) tail shortening step; (1) the accumulation of long poly(A) tails in a steady-state and (2) a reduction in the rate of deadenylation. These results demonstrate that eRF3 is involved in the regulation of deadenylation and decay of mRNA through interaction with PABP.[20] Moreover, translationally inactive mRNA with a stem-loop structure upstream of the translation initiation codon was not affected by the eRF3 lesions, suggesting that eRF3 regulates mRNA stability together with translation.[20] Thus, eRF3 not only forms a complex with eRF1 to regulate translation termination, but also regulates the deadenylation and decay of mRNA through its interaction with PABP in a manner coupled to translation.

INITIATION MECHANISM OF mRNA DECAY

The findings denoted above raised important questions about which of the deadenylases is involved in the eRF3-mediated deadenylation and how eRF3 activates the deadenylase(s). As described above, poly(A) tail shortening is mediated by the two major mRNA deadenylases Pan2–Pan3 and Caf1–Ccr4. In yeast, Pan2–Pan3 catalyzes the first trimming of about 20 nucleotides from the 3′ end and Δpan2 shows the accumulation of mRNA with long poly(A) tails. Meanwhile, Caf1–Ccr4 is responsible for the deadenylation/decay rates of mRNA and Δccr4 is characterized by a reduced rate of deadenylation. Lesions of eRF3 have the phenotype of both a long poly(A) tail of steady-state mRNA and reduced rates of deadenylation/decay of mRNA, indicating that eRF3

stimulates both Caf1–Ccr4 and Pan2–Pan3 deadenylase complexes.[21]

The same is true in mammalian cells. Interestingly, biochemical analysis revealed that not only eRF1–eRF3[18,21] but also Pan2–Pan3[21,39,40] and Caf1–Ccr4[21,41–43] bind to PABP, in which the eRF3, Pan3, and an anti-proliferative protein Tob in each complex all contain a PABP-interacting motif (PAM2) and make contact with PABP. As expected from the structure, eRF1–eRF3 competitively binds to PABP with Pan2–Pan3 and Caf1–Ccr4, and the translation inhibitor cycloheximide inhibits binding of the deadenylase complexes to PABP, suggesting that upon the release of eRF1–eRF3 from PABP during or after translation, the two deadenylase complexes bind to PABP.[21,43] Also, both Pan2–Pan3[39] and Caf1–Ccr4[21] are directly activated by the binding of PABP.

From these results we have proposed a model for the initiation of mRNA decay[21] (Figure 5). After translation termination, the termination complex eRF1–eRF3 dissociates from PABP bound to the poly(A) tail, and in turn, either Pan2–Pan3 or Caf1–Ccr4 associates with PABP, which leads to the activation of the deadenylases and shortening of the poly(A) tail. Consistent with our model, Bedwell's group demonstrated that Tpa1 (*t*ermination and *poly*a*d*enylation) encoding putative prorylhydroxylase interacts with eRF3 and PABP to modulate deadenylation by Pan2–Pan3 and Caf1–Ccr4.[44]

INITIATION MECHANISM OF SPECIFIC mRNA DECAY

The half-lives of mRNA vary from minutes to hours, and transcript-specific half-lives are largely determined by the rate of deadenylation. In the course of investigating the mechanism of mRNA deadenylation, Tob was found to be involved in the general mechanism of mRNA decay.[21] Tob is a member of the anti-proliferative Tob/BTG (for transducer of ERBB2/B-cell translocation gene) protein family, and is involved not only in cell-cycle regulation, but also in spermatogenesis, embryonic development, osteogenesis, T-cell activation, and learning and memory. While these biological activities are not explained by the role of Tob in general mRNA decay, Tob was also found to interact with sequence-specific RNA-binding proteins, CPEB and CPEB-like proteins.[45] CPEB is a cytoplasmic polyadenylation element-binding protein, which specifically recognizes U-rich cis-acting sequence elements in the 3′UTR of specific mRNAs, and CPEB-like proteins are designated CPEB2, CPEB3, and CPEB4. Tob binds to the carboxy-terminal RNA-binding region of CPEB3, mediates recruitment of Caf1 deadenylase to the target of CPEB3, AMPA glutamate receptor (GluR2) mRNA, and negatively regulates its expression.[45] Thus, Tob's role in learning and memory appears to be explained at least in part by regulating the expression of the AMPA receptor. In addition, Tob also regulates the CPEB-target, c-myc mRNA. As in the case of the CPEB3 target, Tob negatively regulates c-myc proto-oncogene expression by recruiting Caf1 to the mRNA and accelerating deadenylation and decay of the mRNA in serum-starved quiescent cells. When cells are stimulated by serum, the Tob–Caf1 deadenylase complex is released from CPEB and c-myc mRNA is stabilized and expressed as an 'immediate-early gene' (our unpublished results). Thus, Tob has a dual role in mRNA deadenylation, acting as both a general regulator via PABPC1 and a transcript-specific

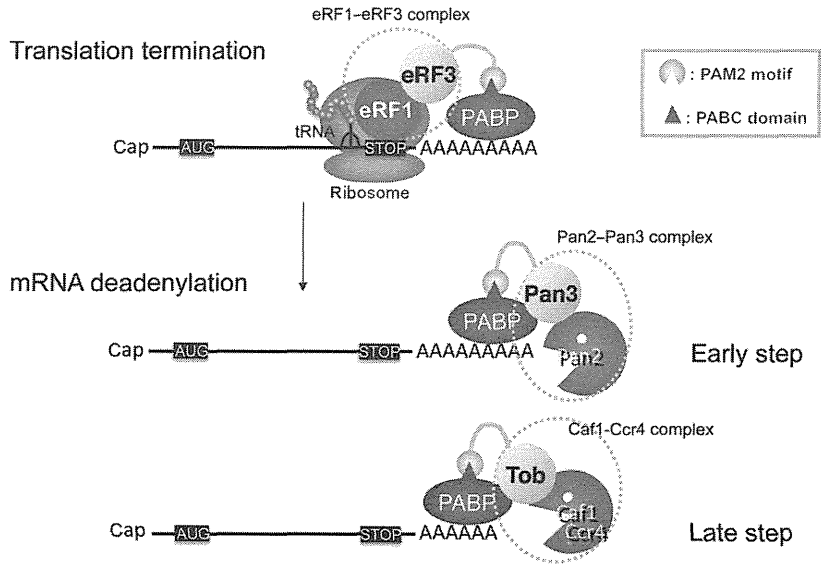

FIGURE 5 | Proposed model for the initiation of mRNA decay. The translation termination factor eRF3–eRF1 and the two major mRNA deadenylase complexes Caf1–Ccr4 and Pan2–Pan3 have poly(A)-binding protein (PABP)-binding motifs (PAM2) in common and competitively bind to PABP. After or during translation termination, eRF1–eRF3 dissociates from PABP bound to the poly(A) tail, and in turn, Pan2–Pan3 or Caf1–Ccr4 associates with PABP. This leads to the activation of the deadenylases and thus the poly(A) tail is shortened during translation. Although multiple PABP molecules are associated with the poly(A) tail, the illustrated model is simplified by drawing the only one PABP molecule.

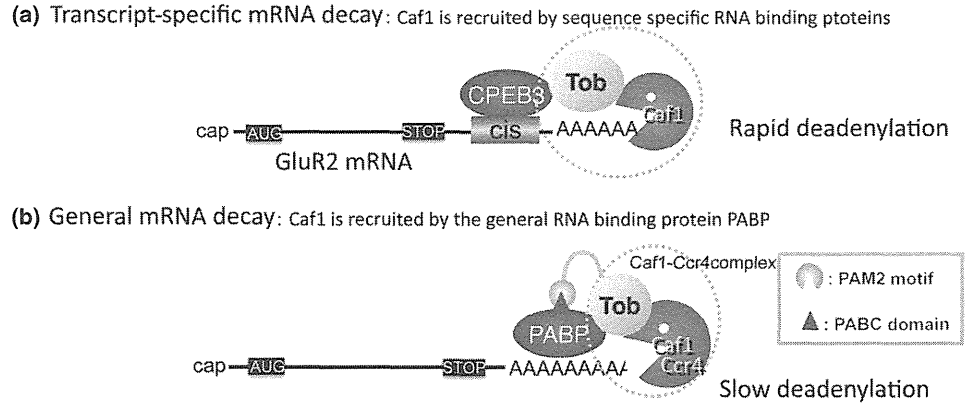

FIGURE 6 | Initiation mechanism for transcript-specific mRNA decay; Tob-mediated mRNA decay. In most mRNA, Tob mediates recruitment of Caf1–Ccr4 to the general RNA-binding protein PABP, and translation termination triggers the recruitment and slow deadenylation. In transcript-specific mRNA decay, however, Tob mediates recruitment of Caf1 deadenylase to the sequence-specific RNA-binding protein CPEB to negatively regulate its gene expression by accelerating deadenylation. As illustrated by the CPEB-target mRNA, cis-acting elements in the 3′ untranslated region and their trans-acting factors can dominantly regulate the half-life of the mRNA.

regulator via CPEBs (Figure 6). As is always the case for regulated mRNA decay, the transcript-specific regulation by Tob via interaction with CPEBs is dominant over the general regulation via PABP; β-globin reporter mRNA with Ms2-binding sites follows deadenylation and decay kinetics of general mRNA, while the same reporter mRNA follows accelerated deadenylation and decay in the presence of Ms2-CPEB.[45]

As illustrated by the regulation of CPEBs-target mRNA, initiation of mRNA decay/deadenylation is specifically modified by cis-acting sequence elements in its 3′UTR, trans-acting RNA-binding proteins, and mRNA decay enzymes (in most cases by recruiting mRNA deadenylases). In many cases, such cis- and trans-acting factors have been reported. First, in Drosophila embryos, a SAM (sterile alpha motif)-domain containing RNA-binding protein, Smaug, which physically interacts with the Caf1–Ccr4 complex, recruits the complex to Hsp83 mRNA to trigger accelerated deadenylation and decay of the transcript.[46] The recruitment-induced enzyme activation was confirmed by tethering Smaug to reporter transcripts. Second, yeast Mpt5, a member of the Puf family of RNA-binding proteins, also recruits the Caf1–Ccr4 complex to HO mRNA to trigger deadenylation of the message.[47] Third, a member of the CELF (CUG-BP, Elav-like family) family of RNA-binding proteins, CUG-BP, specifically binds to GU-rich element (GRE)-containing mRNAs to stimulate poly(A) shortening by recruiting another poly(A)-specific ribonuclease, PARN, to the mRNA.[48] Fourth, KSRP, a KH domain RNA-binding protein, also recruits PARN, as well as the exosome, to the bound mRNA and promotes deadenylation.[49] Fifth, a CCCH-type zinc finger protein, TTP (tristetraprolin), interacts with not only Caf1–Ccr4 but also the exosome and decapping enzyme.[50,51] Both KSRP- and TTP-accelerated deadenylation and decay of the target mRNA are regulated by phosphorylation by p38 MAP kinase. Recent work has dramatically increased our understanding of the molecular basis of the action of miRNA. miRNA binds with argonaute protein (Ago2) and GW182 (TNRC6) to form a RNA-induced silencing complex (RISC) and negatively regulates its target mRNA (reviewed in Ref 52). In this case, the RISC complex also recruits Caf1–Ccr4 deadenylases to the target and accelerates deadenylation of the message.

In contrast to the destabilizing regulation by accelerating deadenylation of the mRNA, some mRNAs are stabilized by retarding deadenylation. α-Globin mRNA is a well-known representative of this type of stable mRNA. α-Globin mRNA has a pyrimidine-rich element (PRE) in its 3′UTR, which is bound by α-complex consisting of αCP. αCP is thought to stabilize mRNA by binding to PABP and repressing the access of deadenylases, or may be by accelerating polyadenylation of the mRNA.[53] Thus, deadenylation, the rate-limiting step of mRNA decay, is a suitable target for the transcript-specific regulation of gene expression.

INITIATION MECHANISM FOR THE DECAY OF ABERRANT mRNA (mRNA QUALITY CONTROL)

In contrast to normal mRNA, aberrant mRNA with structural defects are eliminated by quality control systems. The most well-studied quality control mechanism is nonsense-mediated mRNA decay (NMD).

Nonsense-Mediated mRNA Decay (NMD)

NMD is a surveillance mechanism that accelerates degradation of mRNAs with premature termination codons (PTCs), which likely evolved to protect cells from potentially deleterious truncated proteins produced from the transcripts (reviewed in Refs 54 and 55). Upf1, an RNA-dependent ATPase/helicase, has been identified as a key factor in the NMD pathway. Upf1 interacts with the termination factor eRF3[56] and also with a phosphatidylinositol kinase-related serine/threonine protein kinase SMG1 to form a complex called SURF in higher eukaryotes[57] (Figure 7). When the translating ribosome on nonsense-containing mRNA is stalled at the PTC, the SURF complex binds to the ribosome. SMG1-catalyzed phosphorylation of Upf1, which is essential for triggering NMD, occurs at this stage. Other NMD factors, Upf2 and Upf3, are involved in the exon junction complex (EJC) deposited on the nonsense-containing mRNA, and enhance Upf1 phosphorylation. Although EJCs are usually displaced by the translating ribosome, EJC remains associated with the mRNA downstream of PTC in most but not all nonsense-containing mRNA. The phosphorylated Upf1 then recruits SMG6 and the SMG5, 7 complex, and the nonsense-containing mRNA is subjected to endonucleolytic cleavage by SMG6 and also exonucleolytic degradation.[58–63]

How Is the Termination Codon Recognized as Bona Fide (Normal) or Premature (Aberrant) during Translation Termination?

A number of studies have shown that the positions of nonsense codons affect the intensity of NMD. This phenomenon is called a 'polar effect'. The closer to the 5′ end a nonsense codon is within the coding region, the faster the decay rate of the transcript; the mRNA tends to be degraded by NMD rather than deadenylation-dependent decay.[64,65] Later, it was recognized that the length of the 3′UTR is relevant for eliciting NMD; the distance between the termination codon and the poly(A) tail is critical for determining whether the mRNA is degraded by NMD or deadenylation-dependent decay.[66] (It is not just the linear length of RNA, as RNA forms secondary and tertiary structures.) This notion was supported by the observation that the tethering of PABP near

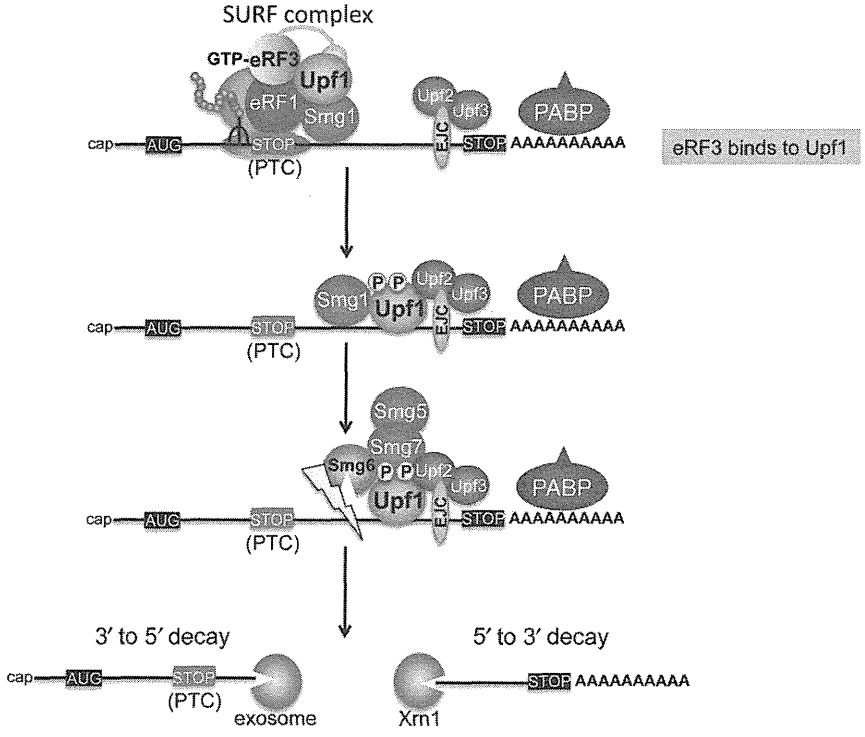

FIGURE 7 | Initiation mechanism for nonsense-mediated mRNA decay. When the translating ribosome reaches the premature termination codon, the termination factors eRF3–eRF1 in complex with Upf1 recognizes the termination codon at the A site of the ribosome. SMG1 catalyzes phosphorylation of Upf1. Exon junction complex, which is usually displaced by the translating ribosome, remains associated with the nonsense-containing mRNA downstream of premature termination codon and enhances the phosphorylation of Upf1. The phosphrylated Upf1 recruits SMG6 to endonucleolytically cleave the message.

the PTC suppresses NMD.[67–72] Interestingly, Lykke-Anderson's group identified PABP as a NMD antagonizing factor.[73] The PAM2 motif of eRF3, which is used for the interaction with PABP, is also used for the interaction with Upf1, and Upf1 competes with PABP for the binding of eRF3. Thus, the distance between the termination codon and poly(A) tail, in other words the interaction between eRF3 and PABP, is important to determine whether the mRNA is degraded by NMD or deadenylation-dependent decay; when the distance between the termination codon and poly(A) tail is great enough to impair the interaction between eRF3 and PABP, Upf1 instead of PABP binds to eRF3 and NMD occurs (the termination codon is recognized as premature), while if the distance is appropriate to allow interaction between eRF3 and PABP, the termination codon is recognized as bona fide and deadenylation-dependent decay occurs (Figure 8).

However, in yeast, it has recently been reported that Upf1 inhibits Pab1 (yeast PABP) binding to eRF3 whereas the interaction between Upf1 and eRF3 is relatively unaffected by Pab1[74] and that Pab1 and poly(A) tail are not required for NMD.[75] Therefore, more than just simple competition between these factors might be involved in activation of the yeast NMD.[74] Moreover, in contrast to the yeast *Saccharomyces cerevisiae*, *Caenorhabditis elegans*, *Drosophila melanogaster*, and plants, where PTC recognition occurs independently of splicing and EJC factors, splicing and EJC factors are known to be involved in the recognition of PTC in mammalian NMD,[54] which also makes the PTC recognition mechanism more complex than the simple competition.

In addition to the role of PABP in the termination codon recognition, PABP also stimulates the activity of eRF3 in translation termination.[76] Thus, the association between eRF3 and PABP is important in defining the termination codon as bona fide to trigger both normal (efficient) termination and the termination-coupled deadenylation.

Nonstop mRNA Decay (NSD)

The second mechanism of mRNA quality control is nonstop mRNA decay (NSD), which was originally described in yeast.[77,78] NSD is a surveillance mechanism that eliminates transcripts-lacking termination codons (reviewed in Refs 79 and 80). The aberrant nonstop mRNA could be generated by premature polyadenylation in the nucleus or by accidental cleavage (RNA damage) within the open reading frame of mRNA. In this system, a member of the eRF3 family, Ski7, plays a central role in triggering the mRNA decay. Ski7 associates with the cytoplasmic form of the exosome and with an auxiliary proteins (Ski2, Ski3, and Ski8) through its amino-terminal domain[24] (Figure 1). When nonstop mRNA is translated by the ribosome, the ribosome is stalled at the 3′ end of the mRNA (Figure 9). In this situation, the stalled ribosome is completely or partially free of codons at its A site. Ski7 is thought to recognize the empty A site by its carboxy-terminal domain. The

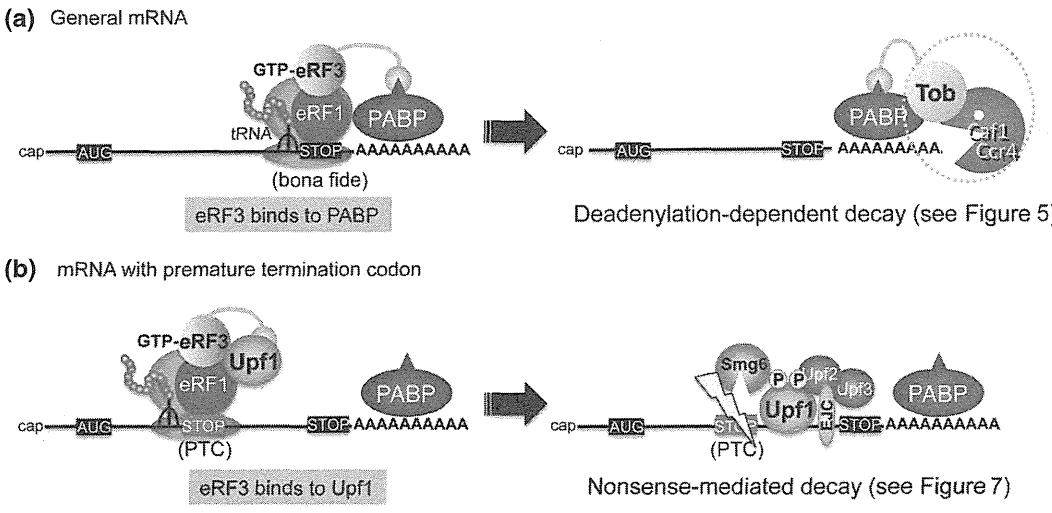

FIGURE 8 | What determines whether translation termination triggers deadenylation-dependent decay or nonsense-mediated mRNA decay (NMD)? (a) General mRNA decay: At the bona fide termination codon, eRF3 can interact with poly(A)-binding protein (PABP), thereby triggering deadenylation-dependent decay (as shown in Figure 5). (b) NMD: At the premature termination codon, which is far from the 3′ poly(A) tail, the interaction between eRF3 and PABP is less efficient. eRF3 thus binds to Upf1 instead of PABP, and triggers NMD rather than deadenylation-dependent decay (as shown in Figure 7).

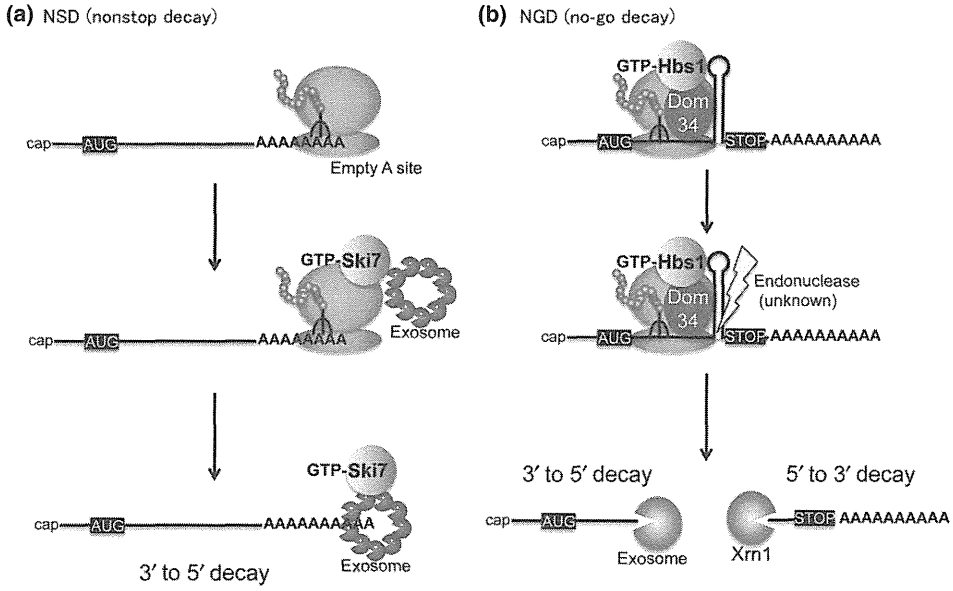

FIGURE 9 | Initiation mechanisms for nonstop mRNA decay (NSD) and no-go decay (NGD). (a) NSD: When a transcript lacking the termination codon is translated, the ribosome enters to translate the 3′ poly(A) tail of the mRNA and stalls at the 3′ end. Ski7 and/or Hbs1-Dom34 recognizes the empty A site of the ribosome, thereby releasing the ribosome. Ski7 recruits exosome to degrade the transcript in the 3′ to 5′ direction. (b) NGD: When a transcript with the structural propensity to cause the ribosome to stall is translated, Hbs1–Dom34 recognizes the A site of the stalled ribosome and the transcript is endonucleolytically cleaved by an unknown nuclease. Hbs1–Dom34 releases the stalled ribosome.

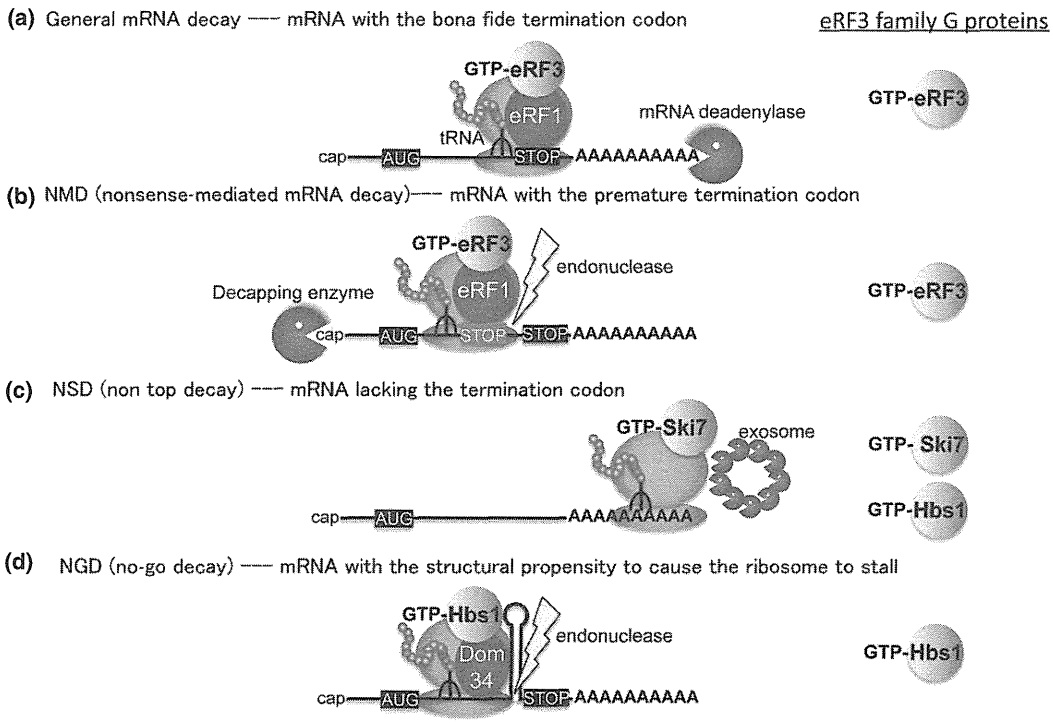

FIGURE 10 | eRF3 family G proteins and mRNA decay. eRF3 family G proteins play key roles in triggering the decay of both general and aberrant mRNAs in a manner coupled to translation termination. In general, eRF3 mediates translation termination at the bona fide termination codon to trigger deadenylation. In nonsense-mediated mRNA decay, eRF3 mediates translation termination at a premature termination codon to trigger endonucleolytic cleavage (metazoa) or decapping (yeast). In nonstop mRNA decay, Ski7 and/or Hbs1 mediate translation termination at the 3′ end of nonstop mRNA to trigger exosome-catalyzed 3′ to 5′ degradation. In no-go decay, Hbs1 mediates translation termination at the stalled ribosome to trigger endonucleolytic cleavage.

proposed model suggests that Ski7 recognizes the 3′ terminus of nonstop mRNA by binding to the stalled ribosome and triggers degradation of the transcript by both releasing the stalled ribosome and recruiting the exosome to the transcript.[78] Thus, nonstop mRNA is degraded from 3′ to 5′ by the exosome. However, Ski7 is found only in a subset of saccharomycete yeasts and no obvious ortholog of Ski7 is present in higher eukaryotes.[81] Among the eRF3 family members, most closely related to Ski7 is Hbs1, which is established as a regulator of NGD [see *No-Go Decay (NGD)* section]. Very recently, Hbs1 was found to be involved in NSD in mammalian cells (our unpublished data) and also in yeast.[82] Thus, Hbs1 is thought to be the responsible regulator of NSD in higher eukaryotes, and Saccharomycete yeasts have evolved a specialized mechanism for NSD in which two eRF3 family members are involved. Hbs1 is the closest relative of eRF3 and forms a complex with Dom34, which is structurally related to eRF1. Recent findings demonstrated that similar to eRF1–eRF3, Hbs1–Dom34 enters the A site of the ribosome and recycles the ribosome to terminate translation in a codon-nonspecific manner.[16,17,82] Although the precise mechanism has not been elucidated, Hbs1 probably functions not only in recycling the stalled ribosome but also in recruiting the exosome to the target mRNA especially in higher eukaryotes (our unpublished data).

No-Go Decay (NGD)

mRNA with structural features that cause the elongating ribosome to stall is eliminated by NGD.[83] Such features include a stable secondary structure, rare codons, and modified bases. The key players identified for NGD are Hbs1 and Dom34.[83] As described above for NSD, Hbs1 and Dom34 form a termination complex to enter the ribosome stalled at the abnormal structures formed on the faulty transcript and trigger recycling of the ribosome as well as endonucleolytic cleavage of the mRNA by an unknown nuclease (Figure 9). Endonucleolytic cleavage of the no-go mRNA leads to the production of two fragments. The 5′ fragment with the stalled ribosome is eliminated by a similar mechanism to NSD.[16,17,82] Hbs1–Dom34 releases the stalled ribosome and the fragment is eliminated mainly from 3′ to 5′ by the exosome. The 3′ fragment is mainly degraded from 5′ to 3′ by Xrn1. Because the endonuclease has not been identified, the precise mechanism leading to the endonucleolytic cleavage is not known at present.

CONCLUSION

eRF3 family G proteins have been shown to regulate initiation of mRNA decay in a manner coupled to translation termination. As summarized in Figure 10, decay of both normal and aberrant mRNAs is initiated by the eRF3 family G protein-mediated translation termination event. In most mRNA, the bona fide termination codon is recognized by eRF3–eRF1 in a complex with PABP and deadenylation-dependent decay occurs. However, in mRNA with a PTC, the aberrant termination codon is recognized by eRF3–eRF1 in a complex with Upf1 and endonucleolytic decay occurs. In mRNA without a termination codon, the empty A site of the ribosome is recognized by Ski7 and/or Hbs1-Dom34 in a complex with the exosome, and the mRNA is degraded exonucleolytically from the 3′ end. In mRNA with a structural propensity to cause the ribosome to stall, the mRNA is recognized by Hbs1–Dom34 and degraded by an endonuclease in corporation with exonucleases. Thus, translation termination is the key event in the initiation of mRNA decay and eRF3 family G proteins play pivotal roles in the process.

Although this review has not dealt with GTPBP1 and GTPBP2, distantly related members of the eRF3 family G proteins, in detail, an interesting finding has recently been reported.[84] GTPBP1 also binds with the exosome and modulates mRNA decay, which is reminiscent of Ski7.[24,25] It was hypothesized that the GTP-bound form of GTPBP1 binds to hnRNPs and recruits the exosome to the target mRNA. As described above, GTPBP1 is evolutionally conserved between human and lower eukaryotes including Neurospora crassa but not *S. cerevisiae*. In sharp contrast to this, Ski7 is conserved only in a subset of saccharomycete yeasts.[81] It is tempting to speculate that GTPBP1 is functionally redundant and functions as a counterpart of Ski7. More study will be required to elucidate the precise roles of GTPBP1/2 in mRNA decay.

ACKNOWLEDGEMENT

This work on the initiation mechanism of mRNA decay was supported by a Grant-in-Aid for Scientific Research on Innovative Areas "RNA regulation" (No. 20112005) from the Ministry of Education, Culture, Sports, Science and Technology of Japan and a Grant-in-Aid for Scientific Research (B) (No. 21370080) from Japan Society for the Promotion of Science.

REFERENCES

1. Bourne HR, Sanders DA, McCormick F. The GTPase superfamily: a conserved switch for diverse cell functions. *Nature* 1990, 348:125–132.
2. Bourne HR, Sanders DA, McCormick F. The GTPase superfamily: conserved structure and molecular mechanism. *Nature* 1991, 349:117–127.
3. Hoshino S, Miyazawa H, Enomoto T, Hanaoka F, Kikuchi Y, Kikuchi A, Ui M. A human homologue of the yeast GST1 gene codes for a GTP-binding protein and is expressed in a proliferation-dependent manner in mammalian cells. *EMBO J* 1989, 8:3807–3814.
4. Hoshino S, Imai M, Mizutani M, Kikuchi Y, Hanaoka F, Ui M, Katada T. Molecular cloning of a novel member of the eukaryotic polypeptide chain-releasing factors (eRF). Its identification as eRF3 interacting with eRF1. *J Biol Chem* 1998, 273:22254–22259.
5. Wallrapp C, Verrier SB, Zhouravleva G, Philippe H, Philippe M, Gress TM, Jean-Jean O. The product of the mammalian orthologue of the Saccharomyces cerevisiae HBS1 gene is phylogenetically related to eukaryotic release factor 3 (eRF3) but does not carry eRF3-like activity. *FEBS Lett* 1998, 440:387–392.
6. Ridley SP, Sommer SS, Wickner RB. Superkiller mutations in Saccharomyces cerevisiae suppress exclusion of M2 double-stranded RNA by L-A -HN and confer cold sensitivity in the presence of M and L-A-HN. *Mol Cell Biol* 1984, 4:761–770.
7. Kudo H, Senju S, Mitsuya H, Nishimura Y. Mouse and human GTPBP2, newly identified members of the GP-1 family of GTPase. *Biochem Biophys Res Commun* 2000, 272:456–465.
8. van den Elzen AM, Henri J, Lazar N, Gas ME, Durand D, Lacroute F, Nicaise M, van Tilbeurgh H, Seraphin B, Graille M. Dissection of Dom34-Hbs1 reveals independent functions in two RNA quality control pathways. *Nat Struct Mol Biol* 2010, 17:1446–1452.
9. Chen L, Muhlrad D, Hauryliuk V, Cheng Z, Lim MK, Shyp V, Parker R, Song H. Structure of the Dom34-Hbs1 complex and implications for no-go decay. *Nat Struct Mol Biol* 2010, 17:1233–1240.
10. Becker T, Armache JP, Jarasch A, Anger AM, Villa E, Sieber H, Motaal BA, Mielke T, Berninghausen O, Beckmann R. Structure of the no-go mRNA decay complex Dom34-Hbs1 bound to a stalled 80s ribosome. *Nat Struct Mol Biol* 2011, 18:715–720.
11. Hauryliuk V, Zavialov A, Kisselev L, Ehrenberg M. Class-1 release factor eRF1 promotes GTP binding by class-2 release factor eRF3. *Biochimie* 2006, 88:747–757.
12. Kononenko AV, Mitkevich VA, Atkinson GC, Tenson T, Dubovaya VI, Frolova LY, Makarov AA, Hauryliuk V. GTP-dependent structural rearrangement of the eRF1:e RF3 complex and eRF3 sequence motifs essential for PABP binding. *Nucleic Acids Res* 2010, 38:548–558.
13. Fan-Minogue H, Du M, Pisarev AV, Kallmeyer AK, Salas-Marco J, Keeling KM, Thompson SR, Pestova TV, Bedwell DM. Distinct eRF3 requirements suggest alternate eRF1 conformations mediate peptide release during eukaryotic translation termination. *Mol Cell* 2008, 30:599–609.
14. Kisselev LL, Buckingham RH. Translational termination comes of age. *Trends Biochem Sci* 2000, 25:561–566.
15. Jackson RJ, Hellen CU, Pestova TV. Termination and post-termination events in eukaryotic translation. *Adv Protein Chem Struct Biol* 2012, 86:45–93.
16. Shoemaker CJ, Eyler DE, Green R. Dom34:Hbs1 promotes subunit dissociation and peptidyl-trna drop-off to initiate no-go decay. *Science* 2010, 330:369–372.
17. Pisareva VP, Skabkin MA, Hellen CU, Pestova TV, Pisarev AV. Dissociation by Pelota, Hbs1 and ABCE1 of mammalian vacant 80s ribosomes and stalled elongation complexes. *EMBO J* 2011, 30:1804–1817.
18. Hoshino S, Imai M, Kobayashi T, Uchida N, Katada T. The eukaryotic polypeptide chain releasing factor (eRF3/GSPT) carrying the translation termination signal to the 3′-poly(A) tail of mRNA. Direct association of erf3/GSPT with polyadenylate-binding protein. *J Biol Chem* 1999, 274:16677–16680.
19. Uchida N, Hoshino S, Imataka H, Sonenberg N, Katada T. A novel role of the mammalian GSPT/eRF3 associating with poly(A)-binding protein in cap/poly(A)-dependent translation. *J Biol Chem* 2002, 277:50286–50292.
20. Hosoda N, Kobayashi T, Uchida N, Funakoshi Y, Kikuchi Y, Hoshino S, Katada T. Translation termination factor eRF3 mediates mRNA decay through the regulation of deadenylation. *J Biol Chem* 2003, 278:38287–38291.
21. Funakoshi Y, Doi Y, Hosoda N, Uchida N, Osawa M, Shimada I, Tsujimoto M, Suzuki T, Katada T, Hoshino S. Mechanism of mRNA deadenylation: evidence for a molecular interplay between translation termination factor eRF3 and mRNA deadenylases. *Genes Dev* 2007, 21:3135–3148.
22. Roy G, De Crescenzo G, Khaleghpour K, Kahvejian A, O'Connor-McCourt M, Sonenberg N. Paip1 interacts with polyA) binding protein through two independent binding motifs. *Mol Cell Biol* 2002, 22:3769–3782.
23. Kozlov G, Gehring K. Molecular basis of eRF3 recognition by the MLLE domain of poly(A)-binding protein. *PLoS One* 2010, 5:e10169.
24. Araki Y, Takahashi S, Kobayashi T, Kajiho H, Hoshino S, Katada T. Ski7p G protein interacts with the exosome and the Ski complex for 3′-to-5′ mRNA decay in yeast. *EMBO J* 2001, 20:4684–4693.

25. van Hoof A, Staples RR, Baker RE, Parker R. Function of the ski4p (Csl4p) and Ski7p proteins in 3′-to-5′ degradation of mRNA. *Mol Cell Biol* 2000, 20:8230–8243.
26. Decker CJ, Parker R. A turnover pathway for both stable and unstable mRNAs in yeast: evidence for a requirement for deadenylation. *Genes Dev* 1993, 7:1632–1643.
27. Schmid M, Jensen TH. Nuclear quality control of RNA polymerase II transcripts. *Wiley Interdiscip Rev RNA* 2010, 1:474–485.
28. Mangus DA, Jacobson A. Linking mRNA turnover and translation: assessing the polyribosomal association of mRNA decay factors and degradative intermediates. *Methods* 1999, 17:28–37.
29. Herrick D, Parker R, Jacobson A. Identification and comparison of stable and unstable mRNAs in Saccharomyces cerevisiae. *Mol Cell Biol* 1990, 10:2269–2284.
30. Beelman CA, Parker R. Differential effects of translational inhibition in cis and in trans on the decay of the unstable yeast MFA2 mRNA. *J Biol Chem* 1994, 269:9687–9692.
31. Hu W, Sweet TJ, Chamnongpol S, Baker KE, Coller J. Co-translational mRNA decay in Saccharomyces cerevisiae. *Nature* 2009, 461:225–229.
32. Garneau NL, Wilusz J, Wilusz CJ. The highways and byways of mRNA decay. *Nat Rev Mol Cell Biol* 2007, 8:113–126.
33. Sheth U, Parker R. Decapping and decay of messenger RNA occur in cytoplasmic processing bodies. *Science* 2003, 300:805–808.
34. Tucker M, Valencia-Sanchez MA, Staples RR, Chen J, Denis CL, Parker R. The transcription factor associated ccr4 and caf1 proteins are components of the major cytoplasmic mRNA deadenylase in Saccharomyces cerevisiae. *Cell* 2001, 104:377–386.
35. Yamashita A, Chang TC, Yamashita Y, Zhu W, Zhong Z, Chen CY, Shyu AB. Concerted action of poly(A) nucleases and decapping enzyme in mammalian mRNA turnover. *Nat Struct Mol Biol* 2005, 12:1054–1063.
36. Tharun S. Lsm1-7-pat1 complex: a link between 3′ and 5′-ends in mRNA decay? *RNA Biol* 2009, 6:228–232.
37. Kobayashi T, Funakoshi Y, Hoshino S, Katada T. The GTP-binding release factor eRF3 as a key mediator coupling translation termination to mRNA decay. *J Biol Chem* 2004, 279:45693–45700.
38. Hoshino S, Hosoda N, Araki Y, Kobayashi T, Uchida N, Funakoshi Y, Katada T. Novel function of the eukaryotic polypeptide-chain releasing factor 3 (eRF3/GSPT) in the mRNA degradation pathway. *Biochemistry (Mosc)* 1999, 64:1367–1372.
39. Uchida N, Hoshino S, Katada T. Identification of a human cytoplasmic poly(A) nuclease complex stimulated by poly(A)-binding protein. *J Biol Chem* 2004, 279:1383–1391.
40. Siddiqui N, Mangus DA, Chang TC, Palermino JM, Shyu AB, Gehring K. Poly(A) nuclease interacts with the C-terminal domain of polyadenylate-binding protein domain from poly(A)-binding protein. *J Biol Chem* 2007, 282:25067–25075.
41. Ezzeddine N, Chang TC, Zhu W, Yamashita A, Chen CY, Zhong Z, Yamashita Y, Zheng D, Shyu AB. Human tob, an antiproliferative transcription factor, is a poly(A)-binding protein-dependent positive regulator of cytoplasmic mRNA deadenylation. *Mol Cell Biol* 2007, 27:7791–7801.
42. Okochi K, Suzuki T, Inoue J, Matsuda S, Yamamoto T. Interaction of anti-proliferative protein tob with poly(A)-binding protein and inducible poly(A)-binding protein: implication of tob in translational control. *Genes Cells* 2005, 10:151–163.
43. Ruan L, Osawa M, Hosoda N, Imai S, Machiyama A, Katada T, Hoshino S, Shimada I. Quantitative characterization of tob interactions provides the thermodynamic basis for translation termination-coupled deadenylase regulation. *J Biol Chem* 2010, 285:27624–27631.
44. Keeling KM, Salas-Marco J, Osherovich LZ, Bedwell DM. Tpa1p is part of an mRNP complex that influences translation termination, mRNA deadenylation, and mRNA turnover in Saccharomyces cerevisiae. *Mol Cell Biol* 2006, 26:5237–5248.
45. Hosoda N, Funakoshi Y, Hirasawa M, Yamagishi R, Asano Y, Miyagawa R, Ogami K, Tsujimoto M, Hoshino S. Anti-proliferative protein Tob negatively regulates CPEB3 target by recruiting Caf1 deadenylase. *EMBO J* 2011, 30:1311–1323.
46. Semotok JL, Cooperstock RL, Pinder BD, Vari HK, Lipshitz HD, Smibert CA. Smaug recruits the CCR4/POP2/NOT deadenylase complex to trigger maternal transcript localization in the early Drosophila embryo. *Curr Biol* 2005, 15:284–294.
47. Goldstrohm AC, Seay DJ, Hook BA, Wickens M. PUF protein-mediated deadenylation is catalyzed by Ccr4p. *J Biol Chem* 2007, 282:109–114.
48. Moraes KC, Wilusz CJ, Wilusz J. CUG-BP binds to RNA substrates and recruits PARN deadenylase. *RNA* 2006, 12:1084–1091.
49. Gherzi R, Lee KY, Briata P, Wegmuller D, Moroni C, Karin M, Chen CY. A KH domain RNA binding protein, KSRP, promotes ARE-directed mRNA turnover by recruiting the degradation machinery. *Mol Cell* 2004, 14:571–583.
50. Marchese FP, Aubareda A, Tudor C, Saklatvala J, Clark AR, Dean JL. MAPKAP kinase 2 blocks tristetraprolin-directed mRNA decay by inhibiting CAF1 deadenylase recruitment. *J Biol Chem* 2010, 285:27590–27600.
51. Clement SL, Scheckel C, Stoecklin G, Lykke-Andersen J. Phosphorylation of tristetraprolin by MK2 impairs AU-rich element mRNA decay by preventing deadenylase recruitment. *Mol Cell Biol* 2011, 31:256–266.

